DANMARKS OG GRØNLANDS GEOLOGISKE UNDERSØGELSE RAPPORT 2008/4

Geochemistry of Mesoarchaean andesitic rocks with epithermal gold mineralisation at Qussuk and Bjørneøen, southern West Greenland

Mineral resource assessment of the Archaean Craton (66° to 63°30'N) SW Greenland Contribution no. 8

Adam A. Garde

GEOLOGICAL SURVEY OF DENMARK AND GREENLAND
MINISTRY OF CLIMATE AND ENERGY

GEUS

DANMARKS OG GRØNLANDS GEOLOGISKE UNDERSØGELSE RAPPORT 2008/4

Geochemistry of Mesoarchaean andesitic rocks with epithermal gold mineralisation at Qussuk and Bjørneøen, southern West Greenland

Mineral resource assessment of the
Archaean Craton (66° to 63°30'N)
SW Greenland Contribution no. 8

Adam A. Garde

GEOLOGICAL SURVEY OF DENMARK AND GREENLAND
MINISTRY OF CLIMATE AND ENERGY

GEUS

Contents

Introduction

The present report presents major and trace element geochemistry of rocks and residual soil samples collected in 2006 within a relict Mesoarchaean andesitic volcanic arc in western Godthåbsfjord, southern West Greenland. The individual study areas are located north and east of the bay of Qussuk and on Bjørneøen (Figs 1, 2). The presently ongoing study of arc-related supracrustal rocks around Qussuk was initiated in 2004 as part of a larger investigation of the primary geological environments of Archaean supracrustal belts in the Nuuk region, with financial support from the Bureau of Minerals and Petroleum in Nuuk (Hollis 2005; Stendal 2007). The relict volcanic arc forms kilometre-scale belts and smaller magmatic enclaves within tonalitic–trondhjemitic orthogneisses and granites in the eastern part of the Mesoarchaean Akia terrane that forms the bedrock adjacent to north-eastern Godthåbsfjord. Garde (2007a) published a general account of the field characteristics, age, general geochemical signature and setting of the relict arc, and the reader is referred to this publication for a general overview.

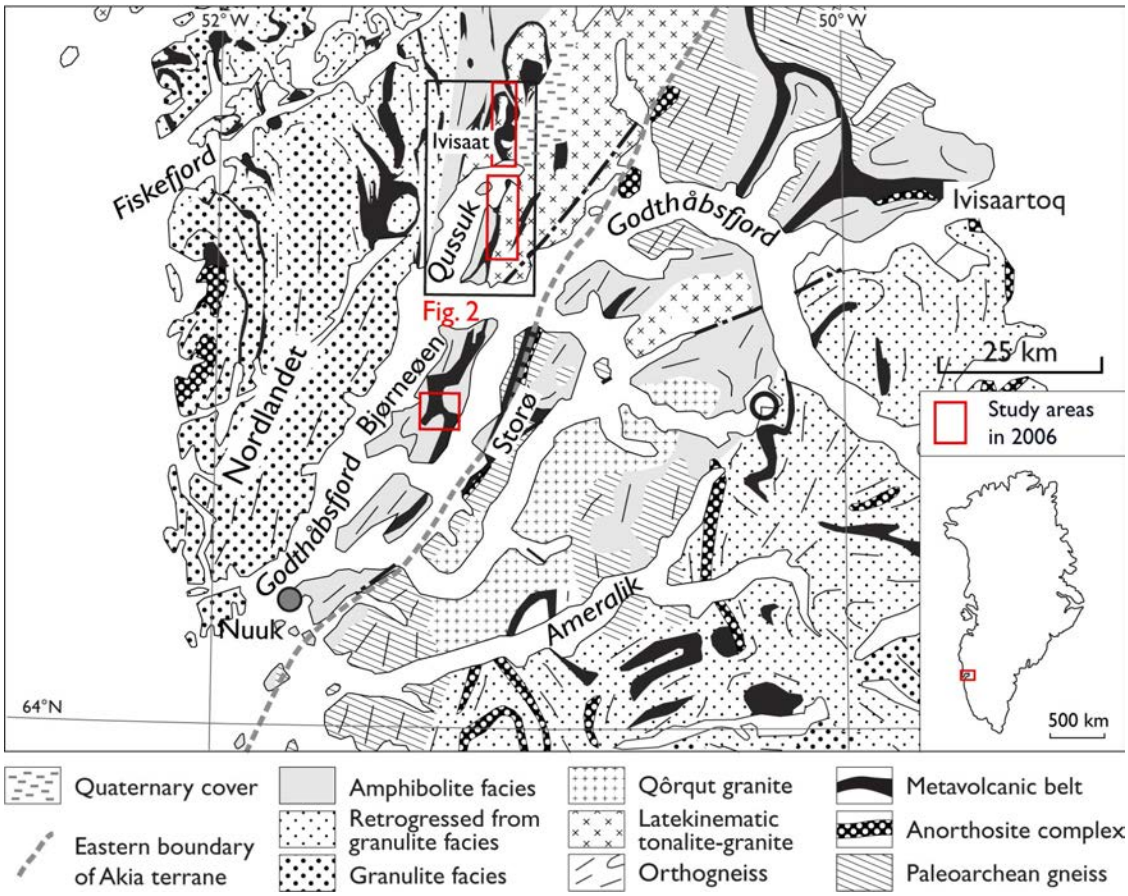

Figure 1. *Geological overview map of the Nuuk region with the study areas of 2006 and the position of Fig. 2. Geochronological sample 488103 was collected at the centre of the red square on Bjørneøen.*

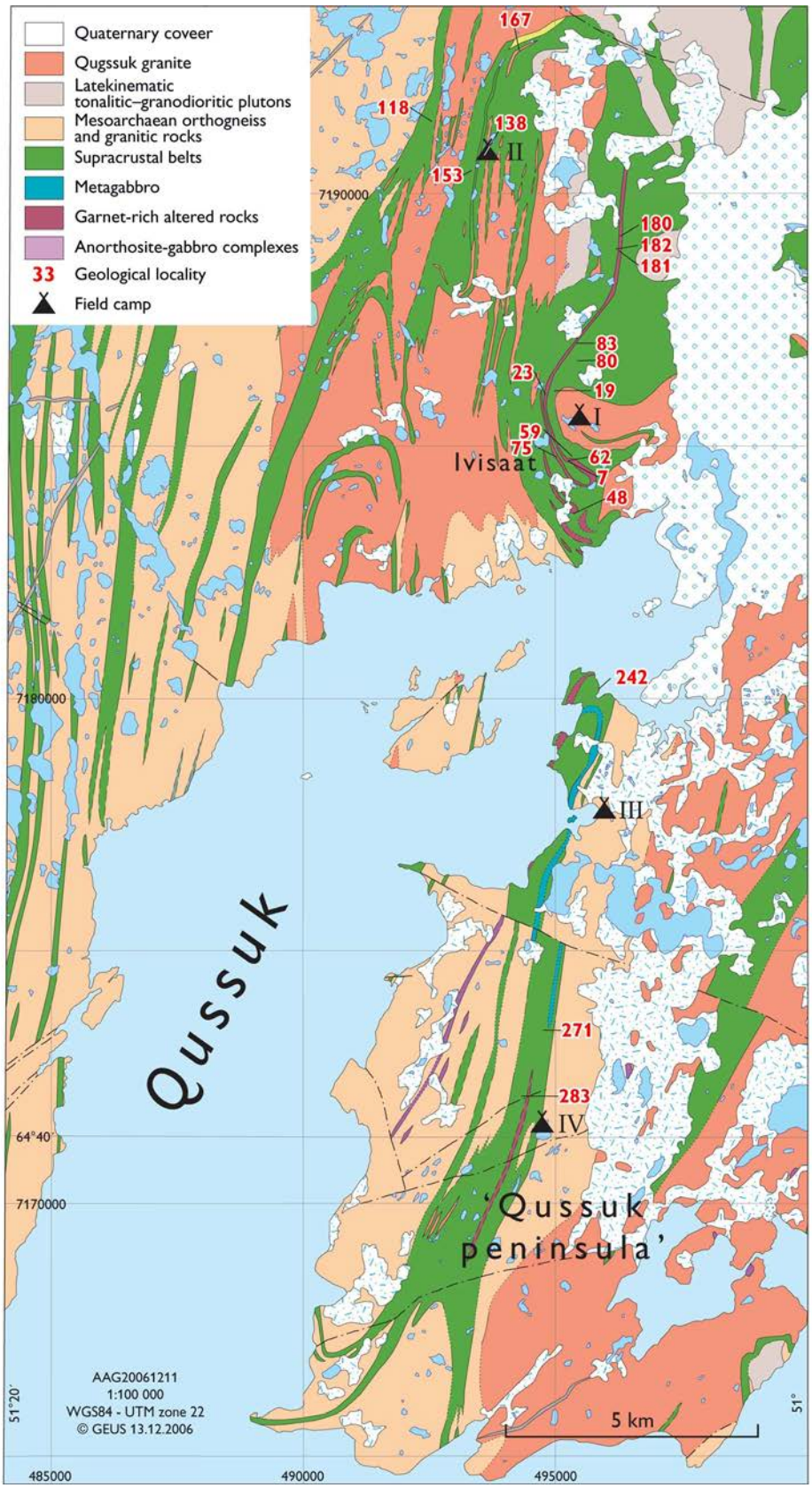

Figure 2. *Geological map of the areas north and east of Qussuk with field localities from 2006 discussed in the text. The map is simplified from Garde (1989).*

Geochemical data from previously collected rocks show that volcaniclastic and associated volcanosedimentary rocks are mainly andesitic in composition; associated metavolcanic and metagabbroic amphibolites are arc-tholeiites (Garde 2007a). A U-Pb age determination of zircon from a volcaniclastic rock at Bjørneøen established a volcanic age of 3071 ± 1 Ma. Zircon from the volcanic belt at the peninsula east of Qussuk, along strike with the belt on Bjørneøen, mainly yielded metamorphic ages of around 2980 Ma. Nevertheless, a few surviving volcanic cores of zircon from the latter area approach the Bjørneøen age in agreement with the obvious field correlation of the supracrustal belt from Bjørneøen to the peninsula. Garde (2007a) concluded that the relict arc represents an early stage in the continental crustal accretion of the Akia terrane in a convergent plate-tectonic setting. It was also noted that although rock complexes that represent the upper, felsic, volcaniclastic parts of such arcs are common in Archaean greenstone terrains worldwide, such complexes are only rarely preserved within the North Atlantic craton of southern Greenland. It was suggested that their near-absence in this craton is not caused by a different geotectonic setting, but is probably due to its generally high metamorphic grade (viz., relatively deep crustal exposure) compared to most other Archaean cratons of the world.

During the field work in 2004 and 2006 it was discovered that hydrothermally altered rocks are widespread in the arc rocks adjacent to Qussuk, and subsequent analytical work showed that the hydrothermal alteration is commonly associated with gold mineralisation in the ppb and locally ppm range (Garde 2005, 2007b; Andreasen 2007). The investigation in 2006 which is the topic of this report was dedicated to further study of the primary volcanic environment of the relict arc and also included an attempt to obtain more information about the age and geological setting of its hydrothermal alteration systems. A couple of key localities were found on a small peninsula in the north-eastern corner of Qussuk and north of Qussuk (Fig. 2), where it was demonstrated beyond reasonable doubt that the hydrothermal alteration took place in unconsolidated rocks prior to deformation and metamorphism, and that the hydrothermal activity was therefore an inherent part of the original volcanic environment (see below). Folded layers up to several metres thick of very peculiar, finely laminated quartz-sillimanite rocks were also discovered within the most intensely hydrothermally altered zones in the arc. It will be demonstrated in this report that these sillimanite-quartz rocks are regionally metamorphosed residual products of intense acid leaching in a volcanic-epithermal, high-sulphidation mineralising system. Field observations from these localities and their interpretations have already been discussed in Garde (2007b) and Garde et al. (2007), but will also be summarised in a subsequent section.

Age of the metavolcanic belt on central Bjørneøen

Garde et al. (2007) briefly discussed the age of the metavolcanic belt on central Bjørneøen, on strike with the belt on the peninsula east of Qussuk, and referred to new geochronological data obtained from sample 488103 in 2007. The full data set from this sample is presented in the following.

Previous age determinations of zircon, purportedly extracted from rocks collected within a couple of hundred metres from each other on central Bjørneøen, yielded very different results (~2825 Ma for sample 479745, Hollis 2005, and 3071 ± 1 Ma for sample 479827, Garde 2007a). Nevertheless, new field observations by the present author in 2006 indicated that the two sample sites belong to the same volcanic belt, and that both the upper and lower flanks of this belt have been intruded by the surrounding, ~3050 Ma orthogneisses (see age determinations in Hollis 2005). A new sample was therefore collected at the locality which had purportedly yielded the ~2825 Ma age data. This sample was analysed in May 2007, see Table 1. The zircon grains are stubby, more or less rounded, mostly only 50–75 microns in length, and very pale pinkish in colour, and on electron backscatter images they display indistinct concentric zonation or are almost homogeneous (Fig. 3).

Table 1. Zircon ion probe U-Th-Pb data from sample 488103, central Bjørneøen

													Ages (Ma)					
Spot #	U ppm	Th ppm	Pb ppm	Th/U measured	f^{206} %	$^{207}Pb/^{206}Pb$	σ %	$^{207}Pb/^{235}U$	σ %	$^{206}Pb/^{238}U$	σ %	Disc. % (conv.)	$^{207}Pb/^{206}Pb$	σ	$^{207}Pb/^{235}U$	σ	$^{206}Pb/^{238}U$	σ
1	553	3	375	0.005	0.01	0.2221	0.17	16.962	1.42	0.5540	1.41	-6.34	2996	2.8	2933	13.7	2842	32.4
2	163	2	113	0.009	0.02	0.2195	0.29	17.199	1.67	0.5682	1.65	-3.19	2977	4.7	2946	16.2	2901	38.6
3	300	8	202	0.026	0.02	0.2140	0.52	16.330	1.50	0.5535	1.41	-4.04	2936	8.4	2896	14.5	2840	32.5
4	184	1	129	0.005	0.02	0.2211	0.24	17.534	1.55	0.5753	1.53	-2.45	2988	3.8	2965	15.0	2929	36.2
5	125	1	89	0.006	0.02	0.2226	0.26	17.774	1.54	0.5790	1.52	-2.29	3000	4.2	2978	14.9	2945	36.0
6	561	7	341	0.012	0.03	0.1887	0.26	13.246	1.93	0.5090	1.91	-3.50	2731	4.3	2697	18.4	2653	41.7
7	95	0	68	0.003	0.05	0.2226	0.28	17.935	1.85	0.5844	1.83	-1.37	3000	4.5	2986	18.0	2967	43.6
8	138	1	99	0.007	0.02	0.2203	0.38	17.748	1.92	0.5844	1.89	-0.66	2983	6.1	2976	18.7	2967	45.0
9	105	3	75	0.027	0.03	0.2206	0.63	17.607	1.54	0.5789	1.41	-1.71	2985	10.0	2969	14.9	2944	33.3
10	81	0	58	0.004	0.03	0.2210	0.41	17.937	1.74	0.5887	1.69	-0.15	2988	6.5	2986	16.9	2984	40.6
11	831	7	588	0.009	0.01	0.2194	0.22	17.507	1.68	0.5788	1.67	-1.34	2976	3.6	2963	16.3	2944	39.5
12	99	1	71	0.005	0.02	0.2209	0.35	17.733	1.66	0.5823	1.62	-1.21	2987	5.6	2975	16.1	2958	38.6
13	118	1	84	0.009	0.02	0.2206	0.25	17.624	1.78	0.5793	1.76	-1.65	2985	4.0	2969	17.2	2946	41.8
14	309	1	220	0.004	0.02	0.2208	0.24	17.787	1.91	0.5842	1.89	-0.88	2987	3.8	2978	18.5	2966	45.2
15	113	1	83	0.005	0.02	0.2200	0.36	18.328	1.51	0.6043	1.47	2.82	2980	5.7	3007	14.6	3047	35.7
16	160	1	114	0.004	0.02	0.2207	0.22	17.756	1.76	0.5836	1.75	-0.92	2985	3.5	2977	17.1	2964	41.7

Errors on ratios and ages are quoted at 1σ level.
f^{206} %: The fraction of common ^{206}Pb, estimated from the measured ^{204}Pb.
Disc. % (conv.): Degree of discordance of the zircon analysis (at the centre of the error ellipse).

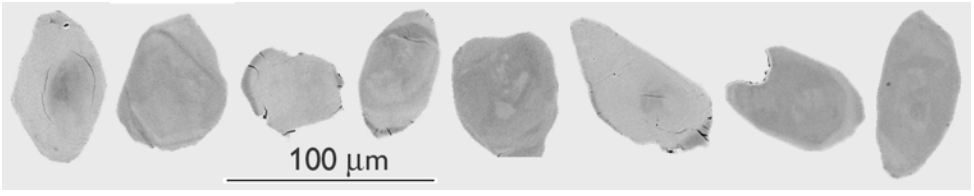

Figure 3. *Electron backscatter images of typical, small, stubby to rounded zircon crystals in sample 488103, central Bjørneøen, yielding a metamorphic age of 2988 ± 4.5 Ma.*

All zircon grains have very low Th/U ratios <0.01. A weighted average $^{207}Pb/^{206}Pb$ age of 2988 ± 4.5 Ma (2 sigma) was obtained from 14 out of 16 analysed spots/grains; the two remaining grains (no. 3 and 6, Table 1) yielded apparent dates of 2936 ± 8 and 2731 ± 4 Ma (1 sigma), probably due to early lead loss. The 2988 Ma age is identical to metamorphic ages of 2970–2990 Ma that were previously obtained from the peninsula east of Qussuk (Garde 2007a), and it is interpreted as metamorphic. Seeing that sample 488103 was collected at the same spot as sample 479745, it can be concluded that the previously analysed zircons which were ascribed to sample 479745 must have been labelled erroneously at some stage during their handling and actually come from another sample. (They probably come from Storø, where this age range was found in several other samples from the same analytical batch; see Hollis 2005). In the light of the field observations from 2006 and the recently published age data from Bjørneøen and the peninsula east of Qussuk (Garde 2007a, b; Garde et al. 2007), the new age data confirm that the metavolcanic belts at Bjørneøen and Qussuk are contiguous with each other and are a little older than the surrounding orthogneisses. This also means that there is no late Archaean thrust stacking at central Bjørneøen such as suggested by Hollis (2005).

Synvolcanic hydrothermal alteration north and east of Qussuk, and on Bjørneøen: field observations

The rock types of the relict volcanic arc, their visible volcanic features, and their hydrothermal alteration patterns, have been described in Garde (2007a, b) and Garde et al. (2007). Some important observations pertinent to the premetamorphic hydrothermal alteration are briefly outlined again below as a background to the presentation of the geochemical data. The arc rocks around Qussuk and on Bjørneøen display two types of rocks that have been subjected to premetamorphic alteration. The first type of alteration is generally thought to be associated with circulation of meteoric water, and resulted in carbonate-impregnated rocks, which in their metamorphic state are diopside- and/or epidote-bearing rocks, such as commonly found in most metavolcanic belts in West Greenland. In the Qussuk and Bjørneøen areas this type of alteration is not related to Au ± Cu mineralisation.

The second type of alteration produced rock types which may superficially be mistaken for aluminous metasedimentary rocks. This type appears to have been controlled by leaching of a large range of major and trace elements and variable addition of LIL elements and iron sulphides. It may be associated with Au ± Cu mineralisation. The two types of hydrothermal alteration may well have been genetically related and operated contemporaneously but in different parts of the same volcanic complex (see discussion).

Figure 4. *Bedded, low-strain, intermediate and mafic metatuffs with graded bedding (foreground) at locality 242 (2006). A primary, essentially undeformed contact between intermediate and mafic metatuff is visible in the background (**red arrow**). Synvolcanic hydrothermal alteration has taken place along a bedding surface in the foreground (**blue arrow**). From Garde (2007b) fig. 9.*

One of the key localities for the second type of alteration occurs in the low-strain hinge zone of an isoclinal, S-plunging synform on a small peninsula in the north-eastern corner of the bay of Qussuk (loc. 242, Fig. 2). The mafic to intermediate volcaniclastic rocks of loc. 242 have been metamorphosed at sillimanite-grade amphibolite facies, and display evidence of local partial melting. Nevertheless, the location in the fold hinge zone has protected tuffaceous bedding and other primary features, which are well preserved throughout this particular locality.

Figure 4 displays tuffaceous beds with graded bedding. A thin, rusty weathering zone of hydrothermal alteration, only *c.* 1 cm thick, can be observed along a primary bedding surface (blue arrow). This narrow hydrothermal zone presumably exploited a good permeability along the premetamorphic, still unconsolidated bedding contact. The zone now encompasses fine-grained metamorphic pyrrhotite and scattered garnet crystals, which are considered to epitomise the original chemical change.

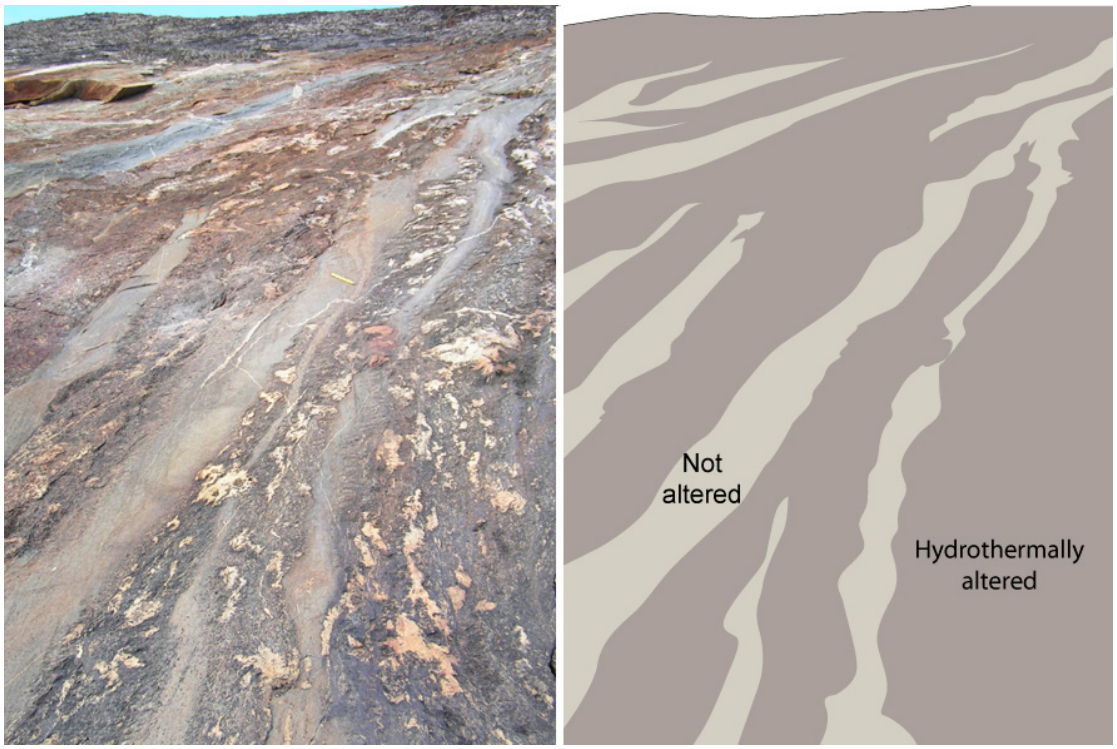

Figure 5. *Grey andesitic metatuff with an interfingering network of rusty weathering, quartz-, garnet- and biotite-rich rocks with partial melt patches. The rocks were leached in a synvolcanic hydrothermal system prior to deformation and metamorphism. Low-strain area in a fold hinge, where the original configuration of the hydrothermal passageways has been maintained. Loc. 242 (2006). From Garde (2007b) fig. 10.*

Figure 5, from an adjacent outcrop at loc. 242 a few metres away, displays an anastomosing, virtually undeformed network of rusty weathering rocks within ordinary grey metatuff. The rusty weathering network is subparallel to the tuffaceous bedding. The rocks within it

are rich in garnet, quartz and biotite, and contain disseminated iron sulphides and patches of partial melting. It can be seen that the surface distribution of unaltered and altered zones is irregular, interfingering, and not the result of folding. However, here and there throughout the outcrops of loc. 242 one can observe a weak foliation and partial melt veins axial planar to the large synform fold, superimposed on the bedding and the partly bedding-controlled distribution of hydrothermally altered zones. Thus, the geometry of the altered rocks mimicks the original hydrothermal vein system prior to deformation and metamorphism. A similar interfingering relationship between unaltered and altered tuffaceous rocks, but much more intensely deformed, can be observed at loc. 83 north of Ivisaat and was described in a previous report Garde 2007b).

The most intensely altered intermediate metavolcanic rocks almost exclusively consist of quartz and sillimanite. These rocks superficially resemble quartzite, and may even be mistaken for pegmatite or granite if only observed from a distance of several metres – that is, they are totally inconspicuous in the field. The sillimanite-quartz rocks have been observed in two places. The largest outcrop is an isoclinally folded layer up to about 10 m thick at the top of Ivisaat mountain (localities 7 and 62, Fig. 2) surrounded by garnet-rich, a little less intensely hydrothermally altered rocks (± sillimanite and cordierite). A second, somewhat thinner, likewise folded layer occurs in the low-lying area below Ivisaat at loc. 48, surrounded by similar garnet-rich rocks as at Ivisaat. It is likely that the two occurrences of sillimanite-quartz rocks were originally formed more or less contemporaneously within the large major hydrothermal alteration system that occurs in the Ivisaat area.

Mineral parageneses in unaltered and altered metavolcanic rocks, and hydrothermal zircon

Inspection of numerous thin sections from unaltered and altered metavolcanic rocks (Appendix A) shows that the unaltered, fresh metavolcanic rocks consist of fine-grained hornblende and/or biotite, plagioclase and quartz in equilibrium with each other, with accessory titanite, apatite, and zircon. Clinopyroxene is only locally present and may partly or wholly be related to early carbonate alteration. Hypersthene is occasionally present in the area north of the head of Qussuk, which thus straddles granulite facies. On Bjørneøen, on the contrary, the metamorphic grade is lower, and the hornblende is blue-green and fine-grained where present. Some thin sections display local or more or less penetrative retrogressive alteration, with growth of fine-grained epidote at the expense of mafic minerals, partial oxidation of iron sulphides, and/or sericitisation of plagioclase (see Appendix A). This type of secondary, retrogressive alteration is not widespread and appears to be completely unrelated to the effects of the main, premetamorphic hydrothermal alteration which is addressed in the following.

Metavolcanic rocks with field evidence of mild premetamorphic hydrothermal alteration such as variably rusty weathering and apparent siliceous character (see the previous section) are indeed characterised by significantly more abundant quartz and less plagioclase than unaltered equivalents. These rocks also contain hornblende and/or biotite, and disseminated iron sulphides, mostly pyrrhotite.

Moderately altered intermediate metavolcanic rocks may be recognised by an elevated quartz content, widely spaced garnet grains up to a few millimetres in size, and commonly small proportions of disseminated iron sulphides. The garnet crystals regularly display poikiloblastic cores and inclusion-free outer parts. The inclusions in the garnet cores are mostly or wholly quartz, biotite, and in some samples also iron sulphides. This observation supports the interpretation that the sulphide mineralisation associated with the hydrothermal alteration took place prior to garnet growth (and thus prior to regional metamorphism). The inspection of thin sections also revealed that these rocks commonly contain cordierite, which is typically associated with biotite and garnet ± quartz in elongate zones up to a few millimetres wide. The cordierite is regularly fine-grained, which probably explains why it was never observed in the field.

Intensely altered intermediate metavolcanic rocks typically contain the paragenesis quartz-biotite-garnet-cordierite-sillimanite, and thus superficially resemble metapelitic rocks at upper amphibolite grade, except that plagioclase is very commonly missing and partial melting generally absent. Zircon and metamorphic rutile are very common accessories. Furthermore, as described above, the contact relationships between unaltered and altered varieties show that these rocks are not of clastic sedimentary origin or the results of kaolinitisation. Sillimanite commonly forms centimetre-sized knots pseudomorphing andalusite, whereas cordierite is very difficult to see with the naked eye, being fine-grained and intergrown with biotite. In most of the cordierite-bearing rocks the cordierite has a characteristic texture with a thin outer zone, in which abundant fine sillimanite needles point inward per-

pendicular to the cordierite grain surface. Sillimanite may also form long prismatic inclusions inside the cordierite.

As stated above, the most extreme hydrothermal alteration resulted in rocks that almost exclusively consist of silica and alumina. In thin section these rocks display a finely laminated texture of interlayered sillimanite and quartz, in places with additional larger clots of sillimanite (probably pseudomorphs after andalusite), besides in places minor white or greenish muscovite (fuchsite). The rocks also contain accessory stubby prismatic rutile, monazite, and in sample 477635 common zircon.

Study of zircon in sillimanite-quartz rock 477635 from Ivisaat
Zircon and monazite grains from sample 477635 have been studied in detail, and U-Pb age determinations as well as U, Th and rare-earth element (REE) analyses on zircon have been carried out by ion probe at the Nordsim laboratory, Naturhistoriska Riksmuseet, Stockholm, Sweden; the full data set will be reported elsewhere. The zircon crystals are short prisms less than 100 microns in length, and have a peculiar texture consisting of three different components (Figs 6, 7).

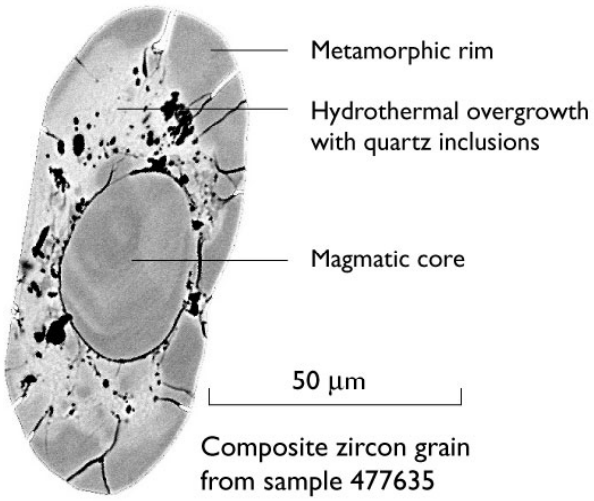

Figure 6. *Backscatter image of typical composite zircon grain from hydrothermally altered rock 477635, now consisting of sillimanite and quartz. The black inclusions in the main body outside the core consist of quartz; black lines are cracks.*

Volcanic, high-Th/U cores with sharp outer boundaries display igneous zonation. The cores are rounded, and their outer surfaces truncate the oscillatory zonation and thus suggest corrosion. The cores are surrounded by main bodies of high-U-Th hydrothermal zircon, which displays heterogeneous U-Th distribution and abundant inclusions of quartz. There are also thin outer rims, which are homogeneous and very low in both U and Th.

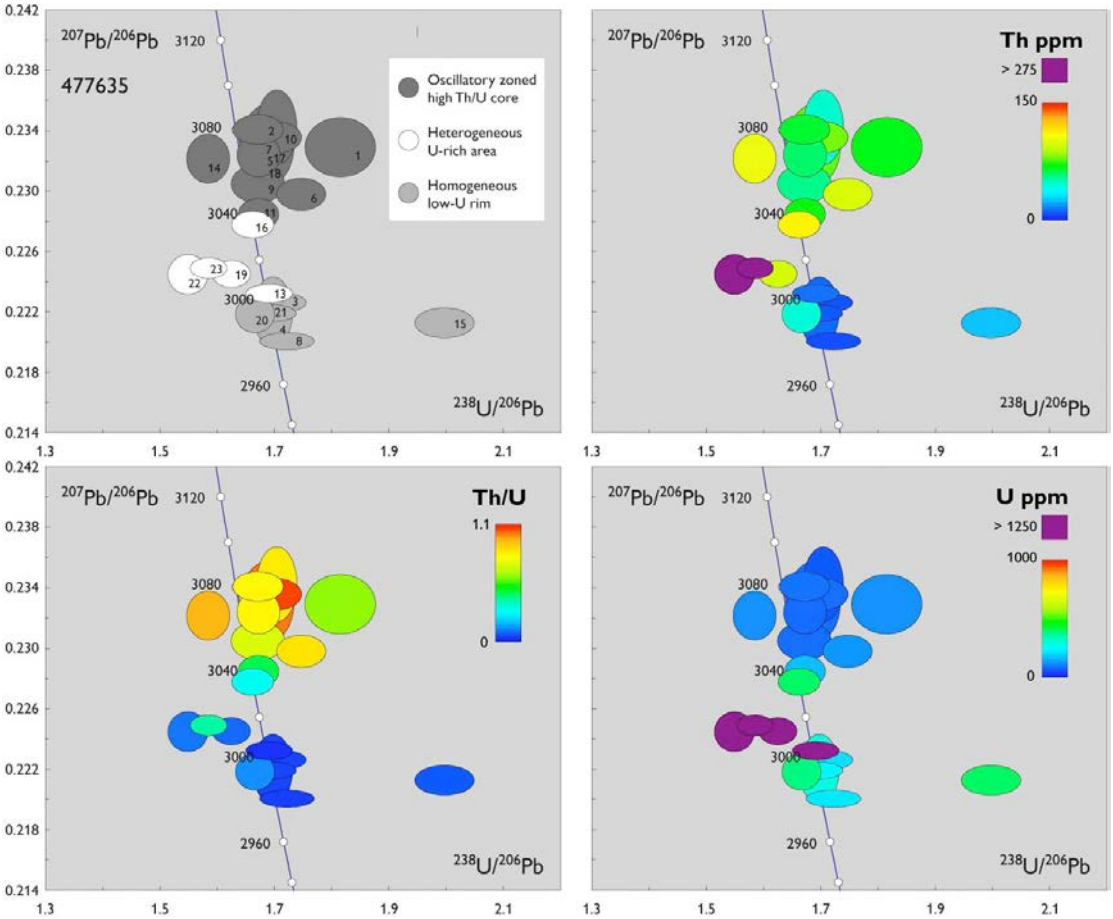

Figure 7. *Graphical representation of ion probe data from zircon in sillimanite-quartz rock 477635. Error ellipses are shown at the 1 sigma level, and age data from the heterogeneous, high-U-Th hydrothermal parts of the zircon crystals are regarded as minimum ages.*

The ages and U and Th distributions are displayed in Fig. 7; the full data will be published elsewhere. The cores yield an overlapping cluster of ages up to 3080 Ma, and their characteristic high Th/U ratios coupled with moderate U and Th contents strongly suggest a volcanic origin. The zircon cores are thus interpreted as volcanic, and their age overlaps with the 3071 ± 1 Ma age of a volcaniclastic rock from Bjørneøen and slightly younger ages of relict cores in metamorphic zircon from volcaniclastic rocks at the peninsula east of Qussuk (Garde 2007a). The main, hydrothermal zircon bodies with their heterogeneous textures yield apparent ages between *c.* 3040 and 3005 Ma, which are regarded as minimum ages; due to the very high U and Th contents early lead loss is considered likely. In fact, these parts may be only slightly younger than the cores. The homogeneous, low-U and Th rims are interpreted as metamorphic. Their age of around 2990 Ma is almost identical to other metamorphic ages previously recorded from the Qussuk area (e.g. Garde et al. 2000) and the same as the metamorphic age of sample 488103 (this report). The monazite grains in sample 477635 are equidimensional and up to a few hundred microns in size. They yield a metamorphic age of *c.* 2985 Ma in agreement with the age data from the zircon rims, dating the main metamorphic event in the Akia terrane; the monazite analytical data will be published elsewhere.

Geochemistry

Analytical procedures

Most samples collected in 2007 were analysed for major and trace elements by Activation Laboratories Inc., Canada; parts of the sample handling and analytical work were performed in Nuuk, Greenland). Most samples were analysed for major elements, Au and trace elements at 'reconnaissance' quality (Appendix B, Appendix D). Some of these samples were reanalysed at 'research grade' for trace elements, using the ICPMS method (Appendix C). Five samples which are rich in trace elements likely to be found in almost insoluble minerals (such as zircon) were also analysed for trace elements at the Geological Survey of Denmark and Greenland, where the ICPMS method was used on solutions from fused glass discs to ensure that trace elements from all mineral phases in the samples were analysed. This independent check showed a good agreement between the two data sets.

Geochemistry of essentially unaltered metavolcanic rocks

Figure 8 displays major element plots of largely unaltered and a few mildly hydrothermally altered metavolcanic rocks collected in 2006 in the Qussuk area and a few on Bjørneøen. The data from 2006 are shown in red, superimposed on data in black from Garde (2007a). There is a large overlap between the two data sets, but also considerable scatter in the new data from samples collected in 2006. Nevertheless, the plots show that the new data set mainly comprises intermediate (andesitic–dacitic) rocks which are generally calc-alkaline in character, besides a few tholeiitic and mafic cumulate rocks (see Garde 2007a for discussion of the original diagrams). The scatter in the data may be due to several factors: the samples have been collected from a large area, they probably include resedimented tuffites besides volcanic flows and tuffs, and weakly hydrothermally altered rocks are included. In their present, deformed and metamorphic state it is difficult to distinguish primary volcanic and volcaniclastic rocks from volcano-sedimentary varieties that have been affected by postvolcanic transport and differentiation, or visually identify relatively minor hydrothermal alteration.

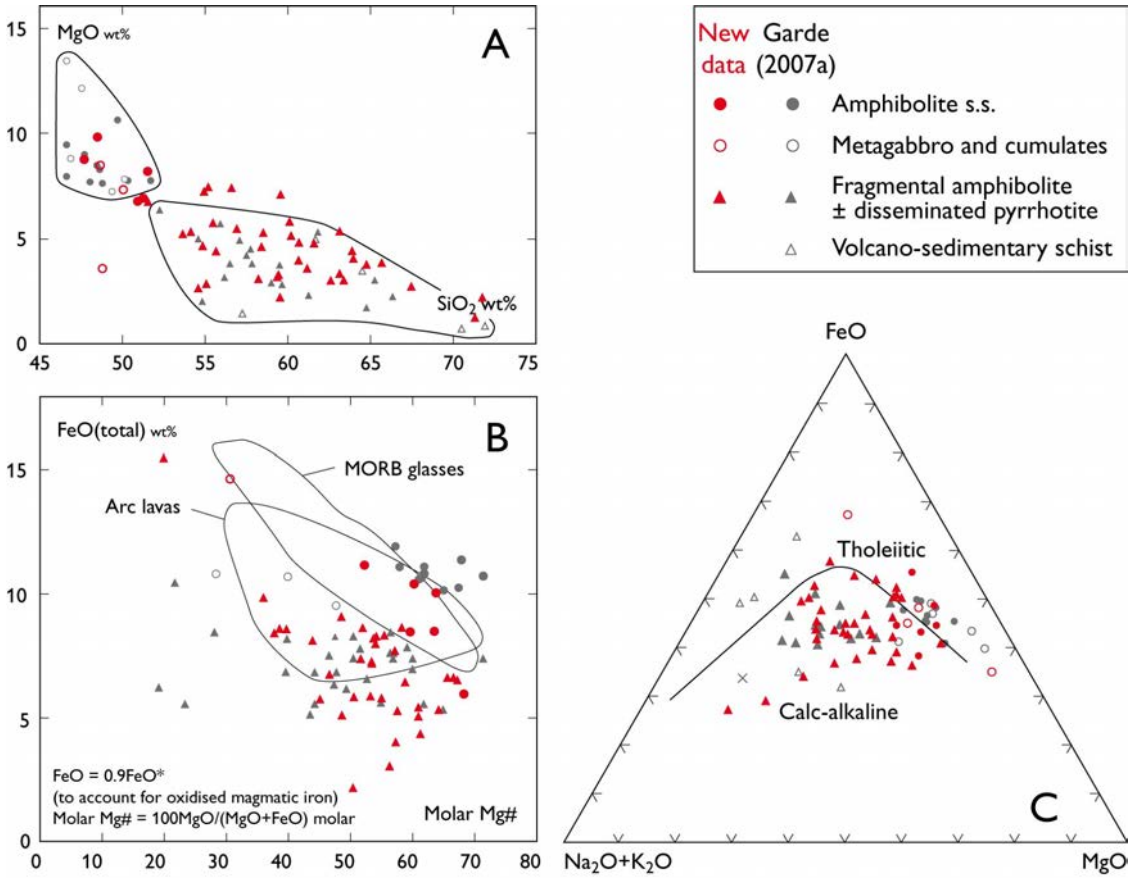

Figure 8. *Major element plots of largely unaltered metavolcanic rocks collected in 2006, mainly in the Qussuk area (besides a couple on Bjørneøen). The new data (shown in red), compared with data from Garde (2007a), confirm the tholeiitic anc calc-alkaline, mainly andesitic compositions of the metavolcanic rocks. The full geochemical data set of unaltered and altered rocks collected in 2006 is shown in Appendix B and C.*

Figure 9 presents chondrite-normalised REE diagrams and mantle-normalised multi-element diagrams of selected samples belonging to the same groups as shown in Fig. 8, again overlain on the older data set from Garde (2007a). The REE diagrams from tholeiitic rocks display flat patterns at around ten times chondrite levels, whereas the intermediate rocks are moderately enriched in LREE. Both the chondrite-normalised REE diagrams and the mantle-normalised diagrams confirm that the metavolcanic belt comprises intermediate, calc-alkaline rocks and arc-tholeiites, which resemble modern subduction-related volcanic arcs.

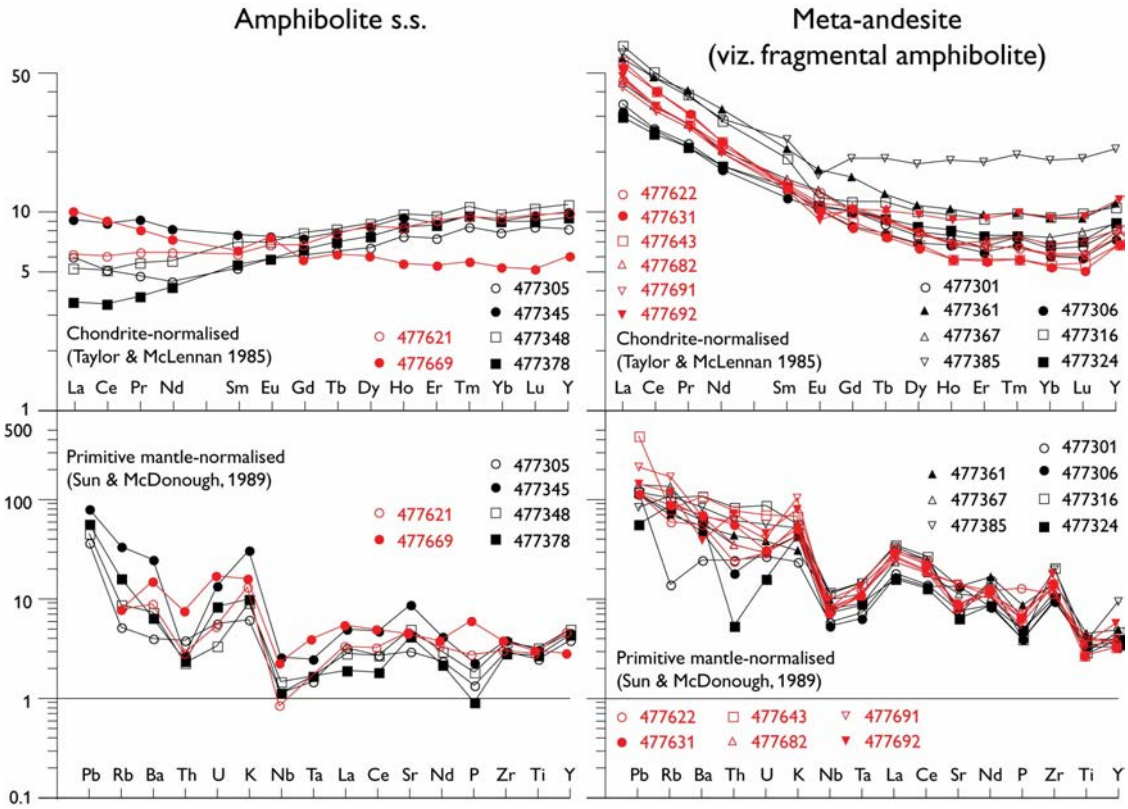

Figure 9. *Multi-element plots of tholeiitic and calc-alkaline, mainly andesitic rocks from the Qussuk area. New data from rocks collected in 2006 are shown in red, and compared with data from Garde (2007a) in black. As expected there is an almost complete overlap between the two data sets. The plotted rocks are considered largely unaffected from synvolcanic hydrothermal activity (except sample 477385 from the data set published by Garde 2007a). The full geochemical data set is shown in Appendix B and C.*

Geochemistry of hydrothermally altered metavolcanic rocks

Geochemical data from hydrothermally altered rocks may be used to determine the gain or loss of individual elements, and not least establish the precise nature of the alteration. However, the treatment of such data can be very complicated. In the Qussuk area, the metavolcanic and volcaniclastic rocks display a range of compositions from tholeiitic to dacitic, which means that the altered rocks cannot be treated as one group. The rocks have furthermore undergone high-grade metamorphism, which may notoriously cause mobility of especially large-ion lithophile (LIL) elements. In addition, there is evidence from the Qussuk area (see below) that elements which are normally regarded as more or less completely immobile, such as Zr and Ga, may in fact have been mobile in some cases. Commonly used procedures, where ratios between assumed immobile elements in altered and unaltered rocks are plotted to monitor the alteration of other elements, may thus be unreliable in the Qussuk area.

For the purpose of this report the chemical effects of the premetamorphic hydrothermal alteration at Qussuk can be assessed in a qualitative way by directly comparing the chemical compositions of unaltered and altered rocks sampled close to each other at individual localities. In this way, only a few samples are dealt with at a time, and uncertainties related to spatial variations in the original magmatic compositions and in the character of the alteration are reduced.

Unaltered and hydrothermally altered rocks north of Ivisaat mountain

Figure 10 shows an example of the appearance and geochemistry of a hydrothermally altered and metamorphosed volcanic rock, and an adjacent, essentially unaltered metatuff. Please note that the photograph of the unaltered rock in Fig. 10A displays thin felsic veins, whereas the actual sample was collected from a homogeneous metatuff without such veins.

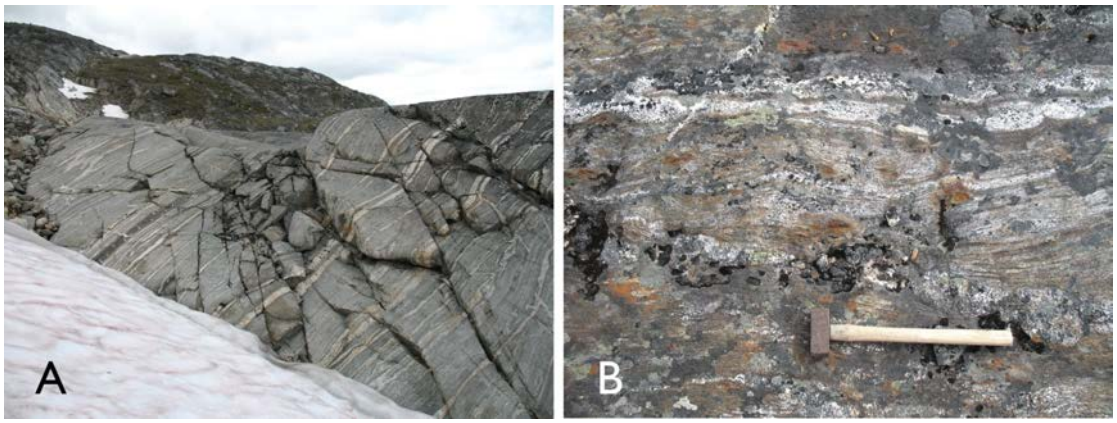

Figure 10. ***A****: Unaltered intermediate metatuff close to loc. 182 (2006) and sample 477677.* ***B****: hydrothermally altered and metamorphosed, garnet-, sillimanite- and cordierite-bearing metavolcanic rock, sample 477676, at loc. 180 (2006).*

Fig. 10B shows a typical outcrop of compositionally layered, rusty-weathering, garnet-sillimanite-rich, hydrothermally altered rock that superficially and in terms of its mineralogy resembles a high-grade metamorphic variety of claystone.

Sample	477677	477676
Locality	182	180
SiO_2	60.34	66.25
TiO_2	0.66	0.78
Al_2O_3	15.17	13.18
FeO*	6.51	9.87
MnO	0.11	0.36
MgO	4.07	4.05
CaO	7.77	0.38
Na_2O	3.10	0.73
K_2O	1.36	3.21
P_2O_5	0.17	0.08
Volatiles	0.56	1.63
Sum	99.28	98.89
V	140	32
Cr	443	2
Co	43	15
Ni	46	4
Cu	15	23
Zn	93	200
Ga	16	26
Rb	62	122
Cs	2.0	1.6
Ba	548	515
Sr	246	26
Y	14.7	65.7
Zr	109	534
Nb	4.2	14.8
La	16.2	57.9
Ce	31.6	114
Pr	3.4	12.5
Nd	13.5	48
Sm	2.75	10.1
Eu	0.921	1.41
Gd	2.54	9.72
Tb	0.43	1.85
Dy	2.64	11.1
Ho	0.53	2.3
Er	1.55	7.27
Tm	0.227	1.11
Yb	1.42	7.14
Lu	0.22	1.11
Hf	2.9	13.8
Ta	0.37	0.78
Pb	7	11
Th	3.21	16.1
U	0.6	1.9

A

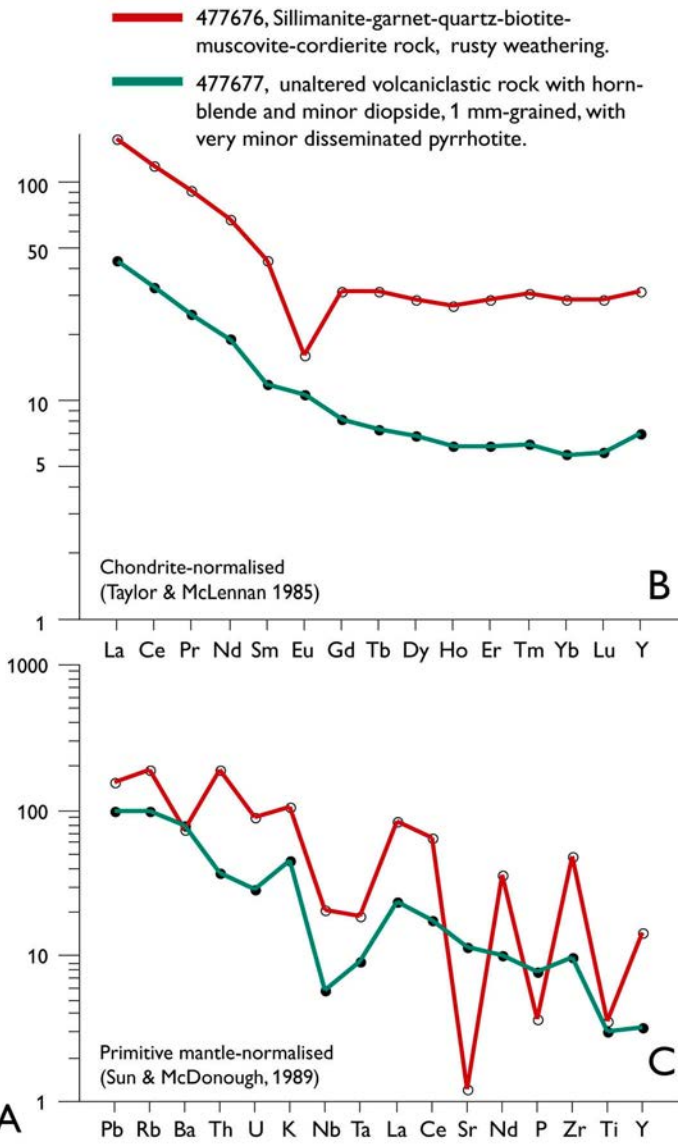

Figure 11. ***A****: chemical compositions of a fresh and a hydrothermally altered rock 5 km north of Ivisaat (oxides of major elements in wt%, trace elements in ppm).* ***B****,* ***C****: REE and multi-element plots. Sample 477677 has patterns typical for intermediate calc-alkaline rocks, whereas ample 477676 has very high overall REE and a strong negative Eu anomaly, indicative of major element depletion in sample 477676 and removal of plagioclase (see main text and discussion).*

In Fig. 11A the altered rock 477676 displays a very substantial apparent enrichment of high field strength (HFS) elements normally regarded as immobile, such as Ti, Nb, Ta, Zr, Hf, all rare-earth and related elements, and Ga. Almost all of the alkaline earth elements Ca and Sr are lost, and Na, P, Ba, as well as the base metals V, Ni, Co, and Cr are significantly reduced. The large-ion lithophile (LIL) elements K, Rb, Pb, Th, and U are enriched, and so are Cu and Zn. The chondrite-normalised REE diagram in Fig. 11B shows a normal, moderately LREE-enriched trend for the unaltered rock 477677 (green line) which is typical for intermediate calc-alkaline igneous rocks with arc affinity. The altered rock 477676 (dark red line) basically shows a very similar trend, but the whole signature is shifted upwards to values approximately three times higher, and there is a prominent negative Eu anomaly

(which corresponds to an absence of plagioclase in the altered rock, see Appendix A). It is also worth noting that the HREE are even more elevated than the LREE. The mantle-normalised multi-element diagram in Fig. 11C displays a prominent zig-zag pattern in the altered sample, corresponding to loss of Sr and P, and variable gain of REE, Nd, Zr, Ti and Y.

Moderately hydrothermally altered rocks at localities 83 and 283

The diagrams in Figs 12 and 13 display REE and multi-element plots of small groups of unaltered and relatively weakly altered rocks collected only few decimetres or metres from each other. These groups of rocks thus provide relative assurance that samples with similar original chemical compositions were collected. Samples 477642–44 come from loc. 83 in relatively strongly deformed metatuffs, but where the interfingering nature of the hydrothermal alteration can still be discerned (see description and fig. 13 in Garde 2007b). The most obvious changes at loc. 83 are loss of alkaline earth elements, Eu and P, and weak enrichment of HFS elements and HREE. the LIL elements display some scatter (which may in part be due to metamorphic element mobility, see discussion).

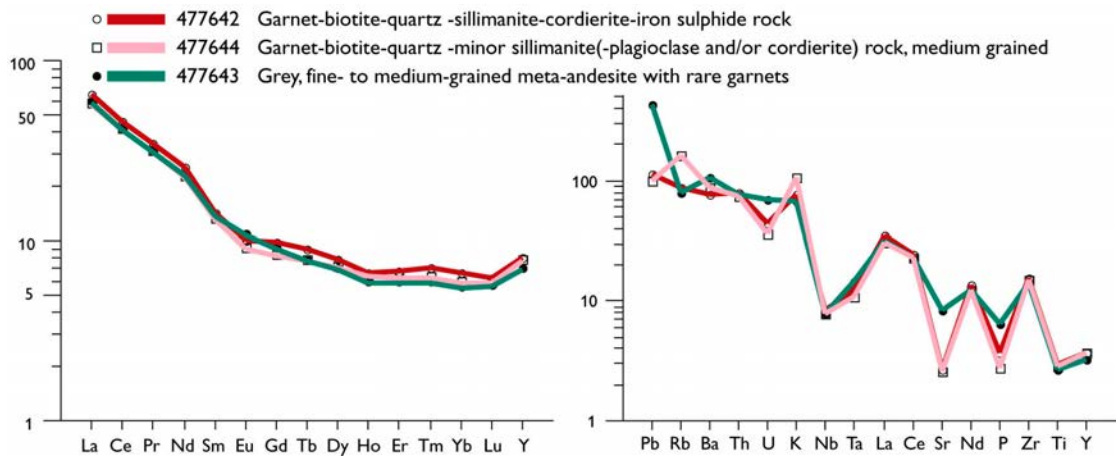

Figure 12. *REE and multi-element diagrams of presumed unaltered and moderately altered andesitic metavolcanic rocks at loc. 83 (2006), displaying loss of especially Sr, P and Eu, and weak enrichment of HREE. This is the locality shown in fig. 13 of Garde (2007b), where an interfingering pattern between unaltered and altered rocks can be observed.*

The two samples from loc. 283 (Fig. 13) display grossly similar patterns, but both samples have negative Eu anomalies, and there is a more noticeable enrichment of HREE.

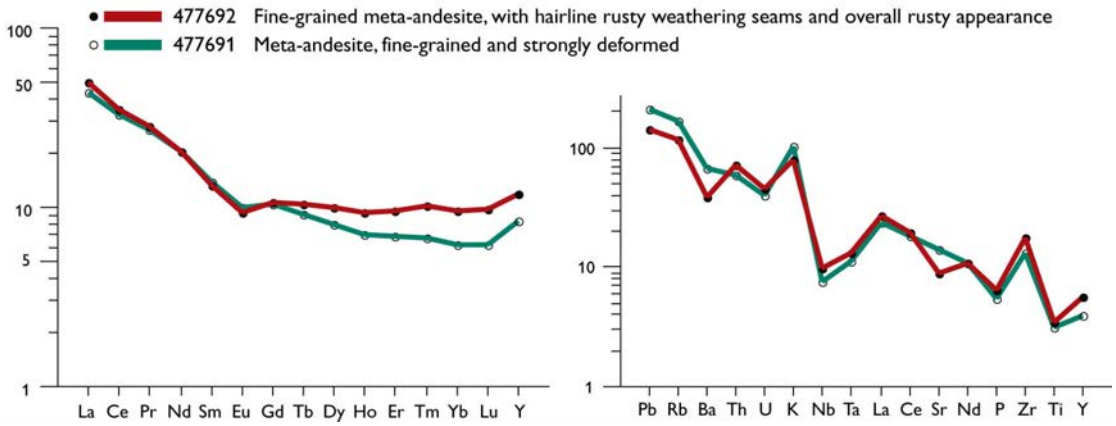

Figure 13. *REE and multi-element diagrams of almost unaltered and moderately altered andesitic metavolcanic rocks at loc. 283 (2006), displaying loss of Sr and enrichment of HREE and HFS elements like Nb, Ta, Zr and Ti. Both samples have negative Eu anomalies; also sample 477691 may be somewhat affected by hydrothermal alteration.*

Moderately hydrothermally altered rocks at localities 19–23 and 59–75

The rocks collected close to each other at localities 19–23 display the same general geochemical patterns (Fig. 14A and B) as the rock pair 477676–77 shown in Fig. 11, with sharp increases in the concentrations of incompatible major and trace elements, development of very strong negative Eu anomalies, and drops in the concentrations of other elements (Appendix B, C). Still other elements appear at roughly constant concentrations in the unaltered and altered rocks. (These elements can also be inferred to have been depleted, due to the large apparent enrichment in immobile elements, see discussion).

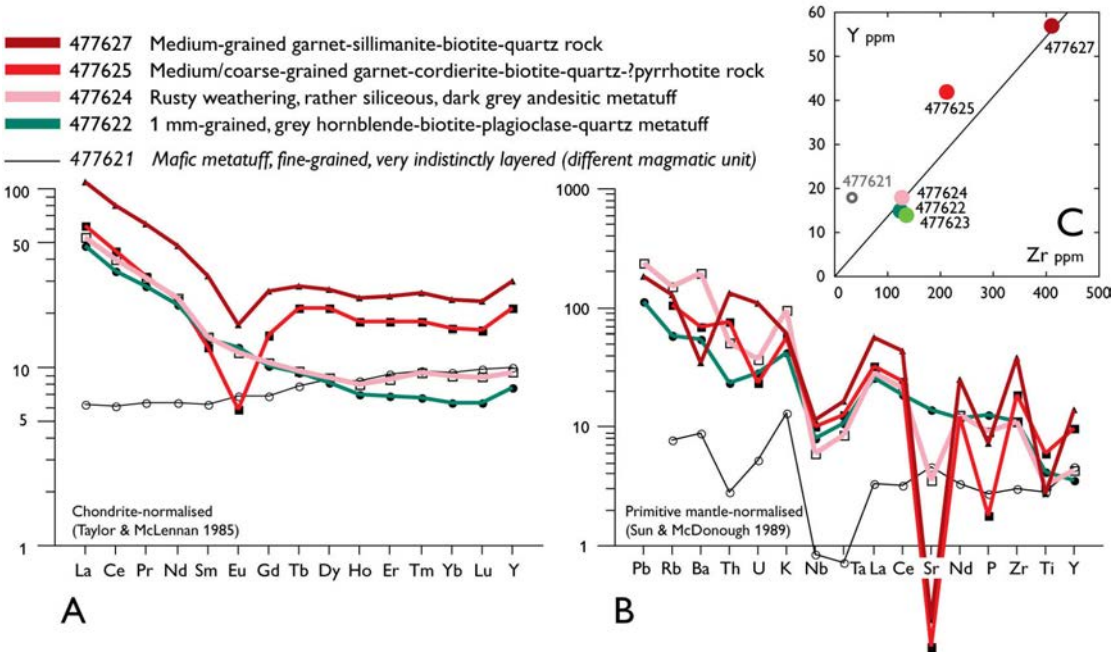

Figure 14. ***A***, ***B****: REE and multi-element plots of unaltered and altered (meta)volcanic rocks from localities 19–23. This series of unaltered and increasingly altered rocks displays the same patterns as the rock pair 477676–77 shown in Fig. 11. The more mafic reference sample 477621 (unaltered, like sample 477622) has a different pattern typical for arc tholeiites.* ***C****: Zr-Y Plot, loc. 19–23. The unaltered and altered samples all plot at or close to a reference line through the origin, suggesting they belong to the same group of intermediate magmatic rocks (except the more mafic reference sample 477621 which plots to the left of the reference line). The two most intensely altered rocks, 477625 and -27, show large apparent gains in both Zr and Y, suggesting substantial depletion of mobile major elements.*

Sample 477621, an unaltered tholeiitic metatuff collected at loc. 19, is included in the diagrams as an independent reference for the sake of comparison. It has a flat REE pattern close to ten times chondrite typical for arc tholeiites, which is different from that of the unaltered intermediate sample 477622 and those of all the other samples enriched in REE.

Fig. 14C is a plot of the two incompatible and generally immobile elements Zr and Y for the same rocks. In this diagram, cogenetic igneous rocks with similar bulk compositions should plot in a close cluster. Bulk enrichment of major elements would move the points towards the origin of the diagram, whereas bulk depletion would move the points away from the origin along a line maintaining the original Zr/Y ratio. Both the unaltered and altered samples do indeed plot at or close to a reference line through the origin, in agreement with the assumption that they belong to the same group of intermediate magmatic rocks. The more mafic reference sample 477621 (shown in black) plots to the left of the reference line and near the origin, also in agreement with the less evolved nature of this rock. The two most intensely altered rocks 477625 and 477627 show large apparent gains in both Zr and Y, suggesting substantial bulk depletion of major elements.

Another group of unaltered and hydrothermally altered rocks was collected at and near the mountain of Ivisaat, including the sillimanite-quartz rock 477635 with its peculiar zircon crystals (which were described in a previous section). Also this group of rocks largely displays the now familiar patterns on REE and multi-element diagrams (Fig. 15). The sillimanite-quartz rock 477635 with the hydrothermally leached and overgrown zircon is an exception. It has 'normal' REE concentrations similar to those found in unaltered rocks (although marginally lower LREE and higher HREE than in the unaltered sample 477631), but it displays a clear positive Eu anomaly. This is discussed below.

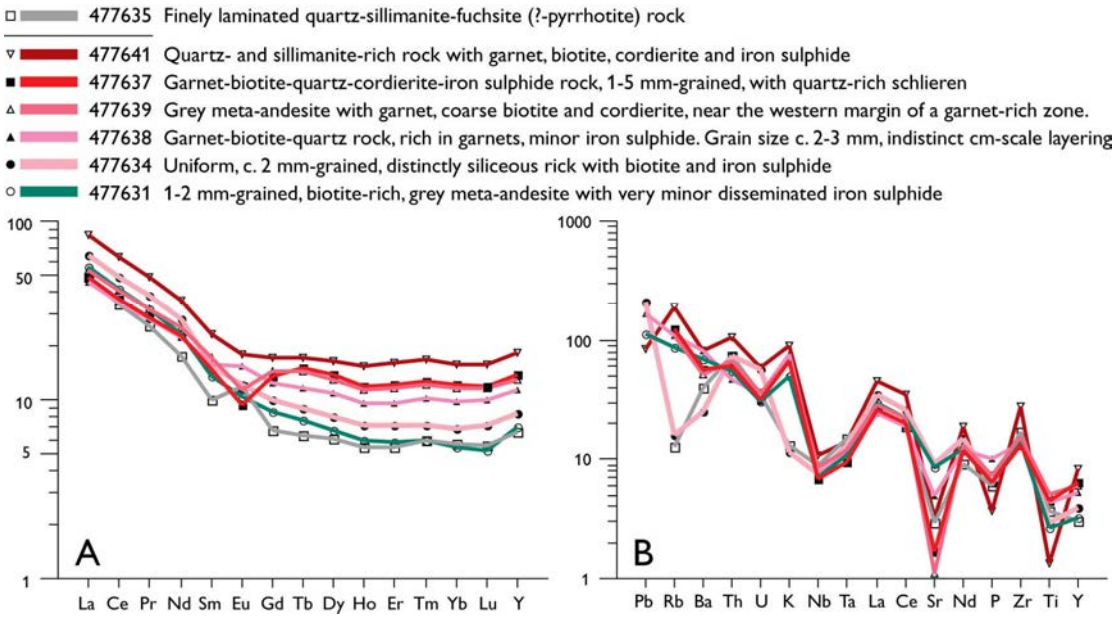

Figure 15. ***A, B:*** *REE and multi-element plots of variably hydrothermally altered (meta)volcanic rocks at Ivisaat. The patterns resemble those in Figs 11 and 12, with a couple of remarkable exceptions in the sillimanite- and quartz-rich samples 477635 and 477637 (see the main text and discussion).*

Fractionation of Ga and Al

Figure 16 is a Ga-Al_2O_3 plot of 32 samples in which both Ga and Al and have been analysed. Most of them plot along a reference line through the origin of the diagram, confirming that Al_2O_3 and Ga are not fractionated in normal crustal environments. However, two samples of sillimanite-quartz rock collected on Ivisaat mountain are depleted in Ga relative to the normal Ga/Al_2O_3 ratio by about 33%. Also a rusty weathering sillimanite-garnet-quartz-biotite-muscovite-cordierite rock, and a silicified amphibolite with disseminated sulphides are enriched in Ga by a similar percentage. A fifth sample 477660, a magnetite-rich layer in metagabbro with 25.37 wt% total FeO and 84 ppb Au, has only 4.28 wt% Al_2O_3 but 74 ppm Ga. This corresponds to more than ten times enrichment of Ga relative to the normal Ga/Al_2O_3 ratio.

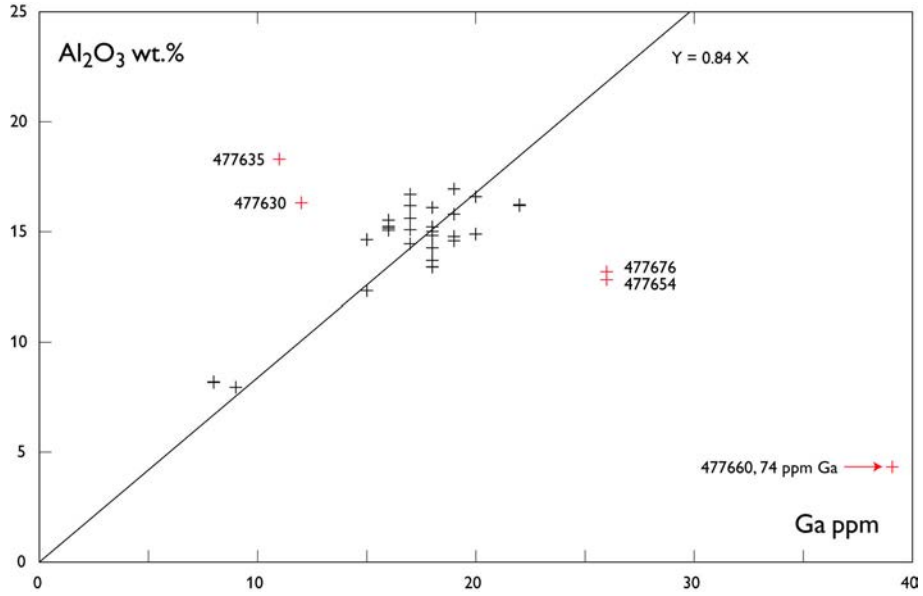

Figure 16. *Ga-Al_2O_3 plot of 32 samples collected in 2006 at Qussuk and on Bjørneøen, for which both Ga and Al have been analysed. A reference line of Al_2O_3 = 0.84 x 106 Ga indicates normal crustal proportions. Intensely hydrothermally altered rocks stand out with aberrant Ga/Al_2O_3 ratios (see the main text and discussion).*

The intense Ga/Al_2O_3 fractionation observed at Qussuk is highly unusual for crustal rocks and may help to characterise the hydrothermal environment in which the alterations took place (see below).

Gold and copper mineralisation

The geochemistry of the rocks collected in 2006 confirm that the hydrothermally altered rocks at Qussuk, as well as their adjacent metavolcanic and volcaniclastic rocks, host gold mineralisation. Gold and copper display positive correlation, whereas arsenic is absent (see below). The gold contents are not striking, except that traces of gold in the ppb range are so commonplace that 15 out of 67 analysed rocks have anomalous Au (20–100 ppb, Appendix B). Besides, 22 residual soil samples collected next to sulphide-mineralised horizons show that gold anomalies are common throughout the study area (Appendix D). Sample 507934 (loc. 83) contains 5.3 ppm Au, and six other soil samples from contain >100 ppb Au (Fig. 2 loc. 80, 118, 153, 167, 271). Garde (2005, 2007a) and Andreasen (2007) have previously described unaltered and hydrothermally altered rocks from the Qussuk area with Au contents in the ppm range, and gold mineralisation is also known from Bjørneøen. Ongoing commercial investigations by NunaMinerals A/S further confirm that there is widespread low-grade gold mineralisation north and east of Qussuk, associated with the hydrothermal alteration zones (R. Christensen and C. Østergaard, NunaMinerals A/S, personal communication 2007, and information from the company's home page).

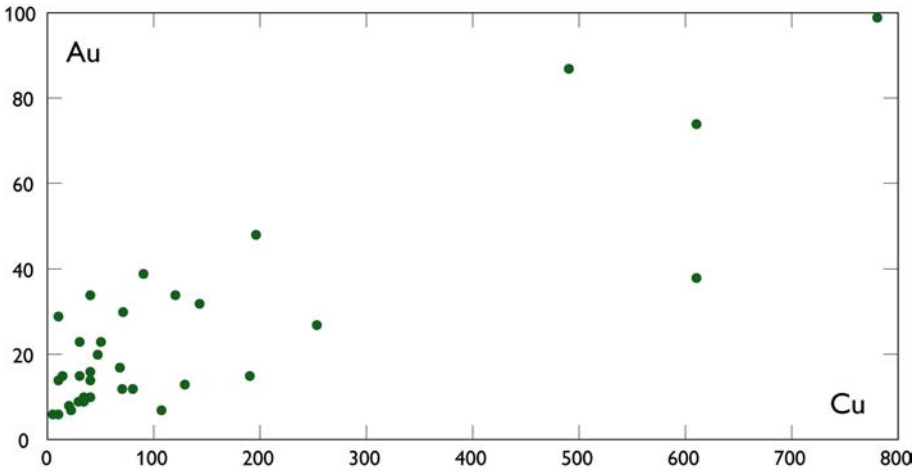

Figure 17. *Correlation of Au and Cu in unaltered and hydrothermally altered metavolcanic and associated rocks at Qussuk.*

Fig. 17 displays the positive correlation between gold and copper (Appendix B). The soil samples contain up to *c.* 550 ppm Cu, but the correlation between gold and copper in these samples (Appendix D) is not as clear as in the rock samples.

Other metals

A few of the copper-bearing samples as well as some other samples contain up to about 550 ppm Zn (see Appendix B), but the correlations between Zn and Au, and Zn and Cu, are not significant. Only trace amounts of Pb have been found. Ultramafic cumulate rocks within the intrusive metagabbroic members of the arc complex contain up to 4000 ppm Cr and 1000 ppm Ni.

Discussion: hydrothermally altered rocks, gold mineralisation, and modern equivalents

Summary of field observations and mineralogical changes in the hydrothermally altered rocks

Two types of hydrothermal alteration were inferred from field observations: one type related to carbonate-impregnated rocks, and a second type related to aluminous rocks with disseminated iron sulphides and associated with gold (-copper) mineralisation. Field observations indicate that both types of alteration occurred prior to deformation and metamorphism.

The mineralogical changes associated with the second, more important type of hydrothermal alteration follow a definite trend which can be summarised as follows. In their current metamorphic state the unaltered intermediate volcanic rocks consist of plagioclase, minor quartz, and biotite ± hornblende. In altered rocks plagioclase and hornblende are lost, and garnet and dispersed iron sulphide (mostly pyrrhotite) appear, as well as commonly cordierite. Besides, the proportions of quartz and biotite increase, and sillimanite appears in rocks affected by more advanced alteration. In the most intensively altered rocks first cordierite and then garnet and biotite disappear, to leave only quartz and sillimanite (besides pyrrhotite and very minor biotite and/or muscovite).

Summary of compositional changes in hydrothermally altered rocks

Summarising from previous sections, the hydrothermally altered rocks display progressive apparent enrichment of HFS elements such as Ti, Nb, Ta, Zr, Hf, rare-earth and related elements, and Ga. Almost all of the alkaline earth elements Ca and Sr are lost, and Na, P, Ba, V, Ni, Co, and Cr are significantly reduced. LIL elements like K, Rb, Pb, Th, and U are enriched, as well as Cu and Zn. Furthermore, the altered rocks display progressively stronger negative Eu anomalies with increasing alteration coupled with their apparent bulk REE gain.

A handful of the most intensely hydrothermally altered rocks display anomalous REE patterns and/or Ga/Al compositions and in some cases anomalous gold concentrations when compared to the rest of the hydrothermally altered rocks. The sillimanite-quartz rock 477635 displays a distinctive positive Eu anomaly, but no apparent REE enrichment. Andreasen (2007) described two intensely hydrothermally altered rocks from the Qussuk area with positive Eu anomalies and low overall REE abundances (both of which contain Au in the ppm range): a quartz-rich rock with 5.1 ppm Au (Andreasen's sample 497686), and a siliceous rock with semi-massive sulphides and 8 ppm Au (497608). In addition, five of the samples collected by the present author display Ga-Al fractionaton, which is very rare in crustal rocks. The two sillimanite-quartz rocks 477630 and 477635 have Ga/Al ratios that are significantly lower than in normal crustal rocks. Besides, sample 477635 is weakly gold

mineralised. Three other altered rocks, two of which are also weakly gold mineralised, have anomalously high Ga/Al ratios. These features are discussed in a separate section below.

The aluminous rocks are not of clastic sedimentary origin

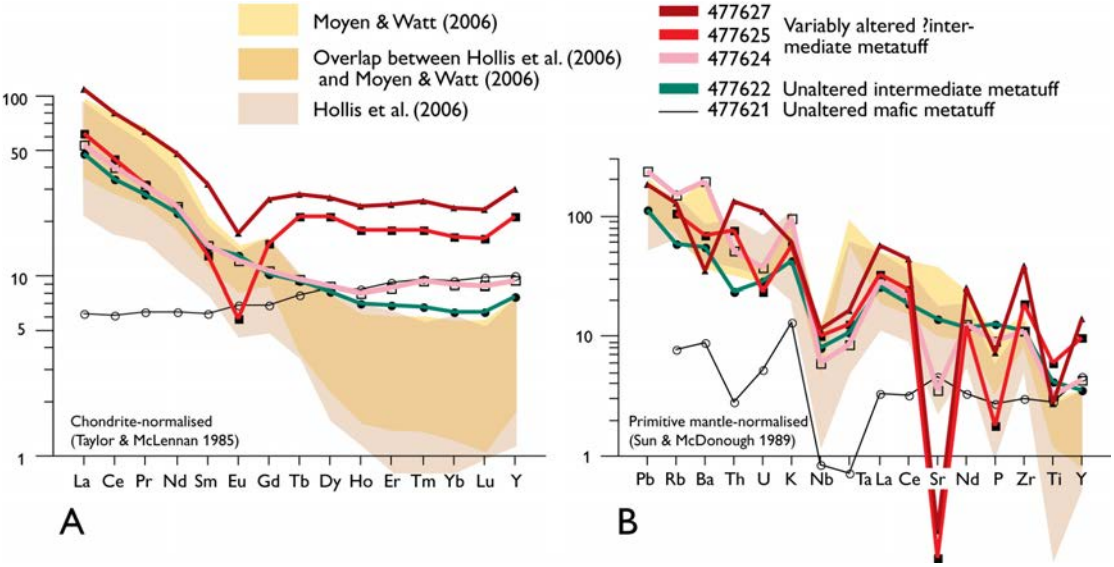

Figure 18. *Comparison between minor and trace element compositions of Archaean clastic sedimentary rocks in central West Greenland (Hollis et al. 2006; Moyen & Watt 2006) and hydrothermally altered metavolcanic and associated rocks at Qussuk.*

Fig. 18 compares the REE and mantle-normalised multi-element patterns of intensely altered metavolcanic rocks in the Qussuk area with two groups of Meso- to Neoarchaean clastic metasedimentary rocks in central West Greenland with siliceous, arkosic and pelitic compositions (Hollis et al. 2006; Moyen & Watt 2006). In the right-hand part of the multi-element diagram (Fig. 18) both groups of rocks display zig-zag patterns, but the positive and negative extremes are much larger in the rocks from Qussuk than in the clastic metasedimentary rocks. Differential loss of especially plagioclase relative to quartz and some heavy minerals during erosion and transport readily explains the moderate zig-zag pattern observed in the detrital rocks from central West Greenland. The zigzag pattern of the rocks from Qussuk is much more pronounced and arguably requires a different explanation, namely severe leaching of mobile elements and corresponding apparent enrichment of immobile elements.

Now turning to the REE patterns, both the hydrothermally altered rocks at Qussuk and the clastic metasedimentary rocks from central West Greenland display relative enrichment of the LREE and cannot be distinguished solely on this basis. However, it is noted that the entire REE spectrum gradually increases in each of the variably altered rock series that were studied in the previous section. Thus, the most significant difference between the two groups lies in the HREE. The clastic metasedimentary rocks from central West Greenland have low HREE compositions which approach mantle values. This is normal for detrital

sedimentary rocks irrespective of metamorphism. On the other hand, the aluminous rocks from Qussuk have strongly elevated HREE. In fact, the HREE compositions of the latter rocks are even significantly higher than those of any probable magmatic sources. The mafic volcanic rocks in the Qussuk area do have HREE concentrations that are higher than found in most clastic sedimentary rocks, but mechanical mixtures of immature erosion products from such rocks and felsic detritus would have significantly lower HREE concentrations than the aluminous rocks in the Qussuk area.

In conclusion, putting the field observations pointing to hydrothermal alteration aside, the chemical compositions of the aluminous rocks in the Qussuk area demonstrate on their own that these rocks cannot be metamorphosed clastic sedimentary deposits, even though some of them possess comparable metamorphic mineral assemblages.

The nature of the hydrothermal alteration and its modern equivalent: low-pressure hydrothermal acid leaching in island arcs

It is evident that the second type of hydrothermal alteration resulted in loss of most major and trace elements to produce rocks which largely or wholly consist of elements that are considered immobile in most geological environments. In addition, the geochemical data indicate that even elements like Al have been mobile in some cases: the most altered samples have REE, Y and Zr concentrations that are up to 4–5 times as high as in normal rocks, whereas their Al content is 'normal' or only slightly elevated. Besides, Al and Ga which are normally considered immobile and geochemically very similar, have been fractionated in four altered rocks.

The only modern geological environment in which large-scale leaching of major and trace elements occurs, is found in the uppermost parts of active andesitic volcanic arcs. Both oceanic and continental arcs in the circum-Pacific ring of fire contain hydrothermal systems, in which oxidised hydrothermal fluids at very low, near-surface pressures and temperatures of around 300°C contain dissociated strong acids such as H_2SO_4, HCl and in some cases HF (Sillitoe & Hedenquist 2003). The low pressure is critical in this context, because otherwise the strong acids in the fluids do not dissociate sufficiently to form appreciable H^+ ion activity. On the surface of such active hydrothermal environments, one may find acid lakes with pH ≤ 3 as well as springs with pH as low as between 1 and 0. A large variety of leach products and precipitates are known from modern hydrothermal environments, such as steam-heated, siliceous 'cap rock', siliceous sinter, and various hydrothermally leached rocks consisting of silica, various clay minerals, Al-hydroxides, and Fe and Ti oxides. The most common mineral species in this particular hydrothermal environment (Thompson & Thompson 1996) are:

illite, $(K,H_3O)(Al,Mg,Fe)_2(Si,Al)_4O_{10}[(OH)_2,H_2O]$;
diaspore, $AlO(OH)$;
kaolinite/dickite, $Al_2\ Si_2O_5(OH)_4$;
andalusite, Al_2SiO_5;
alunite, jarosite, $(K,Na)(Al/Fe)_3(SO_4)_2(OH)_6$;

hematite, Fe_2O_3;
rutile, anatase, TiO_2;
replacive silica: quartz, chalcedony and opal;
residual silica: vuggy quartz.

Combinations of these primary mineral species yield rock compositons dominated by Si, Al, Ti, Fe and K, and absence of Ca and Na, i.e., the same range of chemical compositions as in the hydrothermally altered rocks at Qussuk. Thus, the peculiar chemical compositions of the latter rocks suggest alteration in the near-surface environment of an andesitic arc. This conclusion is obviously in agreement with the field evidence and geochemical and age data from the host rocks, which themselves represent the remnants of an andesitic volcanic arc.

REE, Eu, and Ga/Al anomalies in intensely hydrothermally altered and gold-mineralised rocks north of Qussuk: evidence for two successive hydrothermal events?

As noted above, severely hydrothermally altered, commonly gold mineralised rocks north and east of Qussuk display positive Eu anomalies coupled with low overall REE abundances, and Ga/Al fractionation. In this context it is recalled that the zircon grains in sample 477635 (with these geochemical characteristics) provide compelling evidence of intense premetamorphic hydrothermal activity, with zircon leaching and reprecipitation. Their REE, Eu, Au and Ga/Al characteristics may tentatively be interpreted as evidence for two successive hydrothermal episodes, like in modern high-sulphidation environments where gold mineralisation may take place in during a second hydrothermal episode following initial leaching (see below). During the first episode in the Qussuk area, the rocks were percolated by large volumes of acid fluids which led to major and trace element leaching (and leaching of the volcanic zircon in sample 477635), apparent increase of total REE contents, and development of large negative Eu anomalies related to breakdown of plagioclase. The Ga/Al fractionation, which requires very severe hydrothermal leaching, probably also occurred during the first event. During the second episode, zircon was redeposited in sample 477635 together with quartz, and gold mineralisation occurred.

The low total REE abundances and positive Eu anomalies in sample 477635 and Andreasen's (2007) samples 497608 and 497686 may either be due to extreme leaching during the first hydrothermal episode under specific conditions that would allow all REE except Eu to be removed, or during the second hydrothermal episode by dilution with silica (note the abundant quartz inclusions in the hydrothermal zircon) and preferential deposition of Eu. Andreasen's sample 497608 contains albite which might host Eu^{2+}, but sample 477635 does not. Bau (1991) discussed REE behaviour during neutral to mildly acidic hydrothermal conditions and temperatures of up to 600°C based on thermodynamics. He showed that the Eu^{3+}/Eu^{2+} redox boundary depends on both oxygen fugacity and pH and has a complex behaviour, and concluded that it is very difficult to for hydrothermal fluids to cause REE fractionation unless the fluid/rock ratio is extremely high. Apparently there is no simple and straightforward explanation of the Eu behaviour in the leached rocks at Qussuk, and further discussion of this problem is beyond the scope of the present report.

Conclusions: interpretation of the gold mineralisation at Qussuk and a larger perspective

Gold (-copper) mineralisation in modern arc environments

Many modern andesitic arcs contain economic volcanic-epithermal gold (-copper) deposits, for instance in Japan, the Phillipines, New Guinea, Chile, Peru, and western USA. Those associated with bulk leaching are generally of the high-sulphidation type, which is found more or less directly above a magma chamber that acts as the source of the hydrothermal fluid. Detailed studies of modern gold deposits has shown that the gold ± copper mineralisation, if it occurs, is formed by a second pulse of hydrothermal activity in the same overall system, which may succeed the original leaching process. such gold deposits very commonly also contain iron and copper sulphides (including the As-bearing mineral enargite, Cu_3AsS_4), and are commonly also accompanied by deposition or infiltration of K-rich silicate minerals. The gold mineralisation may occur within the hydrothermally leached rocks themselves or in adjacent wall rocks, where the gold may not be accompanied by visible alteration or sulphide minerals. There are numerous local variations in the metallogeny and mineralogy of modern high-sulphidation environments, and no two deposits are exactly alike. According to Hedenquist (reference), the abundance of As, Cu, and sulphide minerals relative to Au is at least partially controlled by the depth of the magma chamber source, and if the magma chamber is very shallow more or less pure Au deposits may form without co-occurrence of abundant Cu- and As-bearing sulphides.

The gold anomalies north and east of Qussuk in the ppb–ppm range, associated with intensely hydrothermally altered rocks, are interpreted as synvolcanic-epithermal mineralisations of high-sulphidation type. The hydrothermal leaching and (probably immediately subsequent) gold-copper mineralisation took place in a volcanic island-arc environment. The volcanic arc is *c.* 3.07 Ga in age, a few million years older than its tonalitic orthogneiss host, and represents the first stage in the magmatic and tectonic accretion of the main part of the Akia terrane. The gold mineralisation on Bjørneøen appears to be associated with less intensely hydrothermally altered rocks: it may be of intermediate-sulphidation type, and may have been located on the flank of, rather than directly above the original magmatic-hydrothermal centre. The volcaniclastic arc rocks and their gold mineralisation were originally located near the top of the volcanic complex. The preservation of the arc may have been controlled by early tectonic thickening by thrusting and isoclinal folding, and subsequent protection by intrusion of tonalite magmas both below and – importantly in this context – above it. After its initial accretion the Akia terrane was tilted, so that its highest crustal level including the relict arc is now exposed in its south-eastern part (Garde 2007a).

Volcaniclastic (meta)volcanic rocks of intermediate composition and relatively low metamorphic grade are known to exist in several other parts of southern West Greenland and have been described from The Târtoq Group along the fjord Sermiligaarsuk around 61°45´N (Evans & King 1993) and in two unpublished theses from the Ravn Storø and

Grædefjord areas, respectively (Friend 1975, 1976 around 62°40´N, and Wilf 1982 around 63°20´N). Garnet-rich rocks and quartzites within metavolcanic belts, which might turn out to be metamorphosed equivalents of hydrothermally altered volcanic rocks, have been reported from many different places in southern West Greenland and provide a potential for epithermal gold mineralisation. The present author considers that the chance of finding such deposits would probably be best in metavolcanic belts within those sections of the North Atlantic craton that have never been metamorphosed at granulite facies grade and therefore represent the uppermost still preserved parts of the craton.

Very few high-grade metamorphic examples of high-sulphidation alteration systems, with or without direct connections to gold mineralisation, have been reported in the literature, but at least two examples in similar arc-related settings from different periods in the history of the Earth can be noted. (1) The Palaeoproterozoic Enåsen gold deposit is hosted by sillimanite-quartz rocks in a metamorphosed Palaeoproterozoic arc system in northern Sweden (Lundqvist et al. 1986: Hallberg 1994). (2) Kyanite-quartz rocks with accessory fuchsite, rutile and locally topaz occur in an Ordovician metavolcanic arc in Virginia, USA, which hosts several deposits of gold and base metals (Owens & Pasek 2007). In both cases the aluminosilicate-quartz rocks were re-interpreted as metamorphosed rocks of andesitic volcanic origin that have been intensely leached in high-sulphidation (advanced argillic) hydrothermal alteration systems. The kyanite-quartz rocks in Virginia have previously been interpreted as metamorphosed aluminous sandstones, but Owens & Pasek (2007) found strong REE enrichment and severe Ga depletion relative to Al. They also pointed out that no unmetamorphosed clastic sedimentary rocks with appropriate compositions exist in the region (or are considered likely to exist elsewhere). The Neoarchaean, granulite facies challenger Au deposit in south Australia has also recently been interpreted as a metamorphosed epithermal arc-related volcanic deposit (McFarlane et al. 2007). However, the host rocks are garnet-cordierite gneisses, suggesting that the wall rock alteration predating or accompanying the gold mineralisation was not nearly as extreme as in the two former cases.

Acknowledgements

The author thanks Thomas R. Hansen and the staff at the Nordsim laboratory, Naturhistoriska Riksmuseet, Stockholm, Sweden, respectively, for assistance with the geological field work and geochronological study reported in this report.

References

Andreasen, B. 2007: Mineralogical and geochemical investigations of gold-bearing Mesoarchaean supracrustal rocks from the qussuk area, southern West Greenland. Danmarks and Grønlands Undersøgelse Rapport 2007/79.

Bau, M. 1991: Rare-earth mobility during hydrothermal and metamorphic fluid-rock interaction and the significance of the oxidation state of europium. Chemical Geology 93, 219–230.

Evans, D.M. & King, A.R. 1993: Sediment and shear-hosted gold mineralization of the Târtoq Group supracrustals, southwest Greenland. Precambrian Research 62, 61–82.

Friend, C.R.L. 1975: The geology and geochemistry of the preketilidian basement complex in the Ravns Storø area, Fiskenæsset region, southern West Greenland. Unpublished Ph.D. thesis, University of London, 245 pp.

Friend, C.R.L. 1976. Field relationships and petrology of leucocratic schists from the Ravns Storø Group near Fiskenæsset. Rapport Grønlands Geologiske Undersøgelse 73, 81–85.

Garde, A.A. 1989: Geological map of Greenland, 1:100 000, Fiskefjord 64 V.1 Nord. Copenhagen: Geological survey of Greenland.

Garde, A.A. 2005: A mid-Archaean island arc complex with gold mineralisation at Qussuk, Akia terrane, southern West Greenland. In: Hollis, J.A. (ed.) 2005: Greenstone belts in the central Godthåbsfjord region, southern West Greenland. Danmarks and Grønlands Undersøgelse Rapport 2005/42, 180–213.

Garde, A.A. 2007a: A mid-Archaean island arc complex in the eastern Akia terrane, Godthåbsfjord, southern West Greenland. Journal of the Geological Society London 164, 565–579.

Garde, A.A. 2007b: A relict island arc complex with synvolcanic epithermal alteration in western godthåbsfjord, southern West Greenland: field work in 2006 at Qussuk and Bjørneøen. Danmarks and Grønlands Undersøgelse Rapport 2007/20, 13–40.

Garde, A.A., Friend, C.R.L., Nutman, A.P. & Marker, M. 2000: Rapid maturation and stabilisation of middle Archaean continental crust: the Akia terrane, southern West Greenland. Bulletin of the Geological Society of Denmark 47, 1–27.

Garde, A.A., Stendal, H. & Stensgaard, B.M. 2007: Pre-metamorphic hydrothermal alteration with gold in a mid-Archaean island arc, Godthåbsfjord, West Greenland. Geological Survey of Denmark and Greenland Bulletin 13, 37–40.

Hallberg, A. 1994: The Enåsen gold deposit, central Sweden. A Palaeoproterozoic high-sulphidation epithermal gold mineralization. Mineralium Deposita 29, 150–162.

Hollis, J.A. (editor) 2005: Greenstone belts in the central Godthåbsfjord region, southern West Greenland. Danmarks and Grønlands Undersøgelse Rapport 2005/42, 213 pp.

Hollis, J.A., Keiding, M., Stensgaard, B.M., van Gool, J.A.M. & Garde, A.A. 2006: Evolution of Neoarchaean supracrustal belts at the northern margin of the North Atlantic Craton, West Greenland. Geological Survey of Denmark and Greenland Bulletin 11, 9–31.

Lundqvist, T., Willdén, M., Kresten, P. & Sundblad, K. 1986: The Enåsen Au deposit and the Alnö alkaline complex. Sveriges Geologiska Undersökning, Avhandlingar och Uppsatser I A4, Series Ca 67, 22 pp.

McFarlane, C.R.M., Mavrogenes, J.A. & Tomkins, A.G. 2007: Recognizing alteration through a granulite facies metamorphic overprint at the challenger Au deposit, South Australia. Chemical Geology 243 (2007), 64–89.

Moyen, J.-F. & Watt, G.R. 2006: : Pre-Nagssugtoqidian crustal evolution in West Greenland: geology, geochemistry and deformation of supracrustal and granitic rocks south-east of Kangaatsiaq. Geological Survey of Denmark and Greenland Bulletin 11, 33–52.

Owens, B.E. & Pasek, M.A. 2007: Kyanite quartzites in the Piedmont province of Virginia: evidence for a possible high-sulphidation system. Economic Geology 102, 495–509.

Sillitoe, R.H. & Hedenquist, J.W. 2003: Linkages between volcanotectonic settings, ore-fluid compositions, and epithermal precious metal deposits. In: Simmons, S.F. & Graham, I. (eds): Volcanic, geothermal, and ore-forming fluids; rulers and witnesses of processes within the Earth. Special Publication, Society of Economic Geologists 10, 315–343.

Stendal, H. 2007: Summary. In: Characterisation of selected geological environments. Mineral resource assessment of the Archaean Craton (66° to 63°30´N) SW Greenland. Contribution no. 1. Danmarks and Grønlands Undersøgelse Rapport 2007/20, 5–12.

Thompson, A.J. & Thompson, J.F.H. (editors) 1996: Atlas of alteration. A field and petrographic guide to hydrothermal alteration minerals. St. John's, Newfoundland: Geological Assisociation of Canada, 119 pp.

Wilf, C.I.Z. 1982. Geochemistry of grey amphibolites, a part of a supracrustal unit in Grædefjord, north of Qeqertarsuatsiaat (Fiskenæsset) in central South-West Greenland. Unpublished M.Sc. thesis, Århus University, Denmark (In Danish). 145 pp. + appendix.

APPENDIX A. - Samples collected in 2006

Appendix A. Samples collected in 2006

Sample	Loc.	Easting-Northing	Rock description	Thin section
Camp 1, north of Qussuk				
477619	2006aag 006	495255 7184651	Qtz-sill(-?pyrrh) rock with secondary, ?colloform goethite.	
477620	2006aag 007	495272 7184701	Sillimanite-quartz-iron sulphide-?staurolite-?fuchsite rock interpreted as ultra-leached metavolcanic rock.	Qtz - sill-sill felt - mu (minor) - ?staurolite (minor; large 2V ~not mica) - rut - pyrrh.
477621*	2006aag 018	495031 7186154	Fine-grained mafic variety of amphibolite from finely (mm-scale) and very indistinctly layered, otherwise homogeneous unit representative of the mafic metavolcanic component. No signs of alteration.	
477622*	2006aag 019	494976 7186105	1 mm-grained, grey hornblende-biotite-plagioclase-quartz rock, member of the andesitic association, near-homogeneous, un-migmatised, from an area with decimetre-scale compositional layering. Representative.	Hbl >>bt - plag - qtz (uncommon).
477623*	2006aag 020	494898 7186140	Rusty weathering, fine-grained grey meta-andesite, relatively siliceous and rich in biotite. Sampling site shown on photo # 46.	
477624**	2006aag 020	494898 7186140	Rusty weathering, rather siliceous, dark grey meta-andesite/amphibolite s.l. from the most rusty weathering zone, 3 m from sample 477623.	Qtz (abundant) - bt- plag - grt- ?pyrrh - ?orthoamph (altered to bt). The thin section is in a micro-fold hinge.
477625**	2006aag 021	494866 7186090	Medium- to coarse-grained garnet-cordierite-biotite-quartz-?pyrrhotite-bearing rock, apparently affected by hydrothermal alteration. One of several layers c. 10 cm thick.	Grt - bt - crd (±altered) - zircon. Grt is poikiloblastic, with Fe-sulph inclusions. No plag.
477626	2006aag 021	494866 7186090	Fine-grained meta-andesite or hydrothermal rock with patches of coarse bt, a few garnets, and common magnetite (cf. alteration zone at Storø).	Qtz - bt - plag (sericitised) - cpx (partially altered to ep) - opaque (?mag). Polished thin section.
477627*	2006aag 023	494803 7186044	Medium-grained garnet-sillimanite-biotite-quartz rock, un-migmatised, interpreted as leached and metamorphosed andesite.	Grt - sill - bt - qtz - ?mag - rut. Common sill inclusions in qtz. Grt has poikiloblastic cores with qtz - bt - ?rut inclusions.
477628	2006aag 016	495000 7185836	Opx-rich (intrusive) ultramafic rock with c. 1 cm opx crystals, and cpx in the groundmass. Large hand specimen only.	Opx (large poikiloblastic) - cpx - phlog (minor). Many small magnetite grains, also inside opx.
477629*	2006aag 032	495701 7184752	Grey, volcaniclastic meta-andesite	Hbl - bt (many small flakes) - plag (sericitised) - qtz (common).
477630*	2006aag 048	495364 7183665	Quartz-sillimanite-fuchsite rock with crude gneissic foliation on a scale of few millimetres. Interpreted as residual from synvolcanic-epithermal leaching.	Qtz - sill - bt - mu (very minor) - rut (abundant small metamorphic grains). Sill also as needles in qtz, and as pseudomorphs.
477631*	2006aag 059	495339 7184809	1-2 mm-grained, biotite-rich, grey meta-andesite with very minor disseminated iron sulphides.	
477632**	2006aag 059	495339 7184809	1-2 mm-grained, biotite-rich, grey meta-andesite with a few garnets ?0.5 cm large and disseminated sulphides.	Orthoamphibole (aggregates with actinolite overgrowths) - bt - qtz - plag - grt (minor) - ?pyrrh.
477633**	2006aag 060	495251 7184785	Uniform, c. 2 mm-grained, rather siliceous qtz-??plagioclase-biotite-iron sulphide rock with anonymous aspect, presumably hydro-thermally altered, metamorphosed andesite. No garnets.	Qtz - plag - bt - hbl (relict, now orthoamphib-ole) - ?pyrrh. Some plag grains zoned with small ?igneous cores. Retrograde texture.
477634*	2006aag 061	495272 7184770	Uniform, c. 2 mm-grained, distinctly siliceous qtz-??plagioclase-biotite-iron sulphide rock with anonymous aspect, presumably hydro-thermally altered and metamorphosed andesite.	
477635**	2006aag 062	495262 7184726	Finely laminated quartz-sillimanite-fuchsite (?-pyrrhotite) rock, fine-grained.	Qtz - sill - pyrrh - bt - mu (both very minor). Possibly minor crd. Concrdant, 2 mm thick tz-pyrrh layer or veinlet. Polished thin section.

*: Chemical analysis. **: Anomalous gold. Mineral abbreviations: Bt: biotite; cpx: clinopyroxene; crd: cordierite; ep: epidote; grt: garnet; mu: muscovite; opx: orthopyroxene; plag: plagioclase; pyrrh: pyrrhotite; qtz: quartz; rut: rutile; sill: sillimanite.

Appendix A (continued)

Sample	Loc.	Easting	Northing	Rock description	Thin section
477636*	2006aag 063	495219	7184684	Grey meta-andesite relatively rich in garnet c. 1-2 mm-grained, with biotite, and not appearing siliceous. A little disseminated iron sulphide (pyrite?).	
477637*	2006aag 065	495096	7184665	Garnet-biotite-quartz-cordierite-iron sulphide rock, 1-5 mm grained, with ?2 cm thick quartz-rich schlieren (±grt, ±bt).	Qtz - bt - grt - crd - sill - opaque - zircon. Sill inclusions in crd. Grt poikiloblastic cores with qtz and opaques. Abundant sill inclusions at marginal zones of crd.
477638**	2006aag 065	495096	7184665	Garnet-biotite-quartz (-Fe-sulphide) rock rich in garnets, c. 2-3 mm grain size, indistinct cm-scale layering. Interpreted as hydrothermall altered andesitic rock.	Grt - qtz - bt - pyrrh - ?albite (minor, possibly crd) - zircon. Grt with poikiloblastic cores and inclusions of qtz, bt, ?pyrrh. Polished thin section.
477639**	2006aag 074	495020	7184805	Grey meta-andesite with garnet, coarse biotite and cordierite, near the western margin of a garnet-rich zone.	Grt - bt - qtz - sill - crd - plag - opaque. Sill-rich rim zones of crd.
477640*	2006aag 075	495040	7184796	Fine-grained amphibolitic metadyke, post-hydrothermal alteration, but pre-metamorphism and deformation.	Hbl - plag - bt (minor). Hbl has many trains of minute ?oxide exsolutions along crystal structure.
477641*	2006aag 075	495040	7184796	Quartz- and sillimanite-rich rock with minor garnet, biotite, cordierite and iron sulphide, adjacent to thin mafic metadyke.	Qtz - bt - grt - sill - crd (or fsp?, locally fine myrmekite texture) - mu - zircon, opaque. Sill inclusions common in qtz.
477642**	2006aag 083	495415	7187043	Garnet-biotite-quartz -sillimanite-cordierite-iron sulphide rock, medium grained, interpreted as hydrothermally altered and metamorphosed andesite.	Qtz - bt - grt - sill - crd. Sill as very fine-grained matsintergrown with bt, and at crd rims growing perpendicular to its margins, like fibrils.
477643*	2006aag 083	495415	7187043	Grey, fine- to medium-grained meta-andesite with rare garnets, adjacent to sample 477642.	Bt - opx (poikiloblastic, in transformation to orthoamphibole.) - plag >> qtz, ap.
477644**	2006aag 083	495415	7187043	Garnet-biotite-quartz -minor sillimanite(-plagioclase and/or cordierite) rock, medium grained. Hydrothermally altered and metamorphosed andesite.	
Camp 2006-2, inland camp north of Qussuk					
477645*	2006aag 093	496795	7192737	Rust-stained local block of meta-andesite, from the first exposure uphill from loc. 92.	
477646 *	2006aag 094	495966	7196428	Fine-grained, homogeneous meta-andesite.	
477647 *	2006aag 096	496242	7200782	Relatively leucocratic amphibolite with disseminated iron sulphides and quartz veins <1 cm thick.	Hbl - cpx - plag - qtz. Qtz (-plag) veins.
477648	2006aag 100	490513	7198522	Ultrabasic rock, ?dunite, grain size *c.* 2 mm, apparently homogeneous. Large hand sample.	
477649	2006aag 100	490513	7198522	Ultrabasic rock, ?dunite, grain size c. 2 mm. Large hand sample.	Ol, equigranular, many small opaque grains (mag).
477650	2006aag 100	490513	7198522	Ultrabasic rock, ?dunite with magmatic layering. Large hand sample.	
477651 *	2006aag 096	496242	7200782	Fine-grained, apparently layered meta-andesite, from locality with volcaniclastic texture.	
477652 **	2006aag 102	493583	7190860	Opx-hbl-layered, deformed ultramafic rock. Presumably originally mainly consisting of coarse-grained opx. Representative sample.	Opx - cpx (weak pleochroism, 2V ~90°, good cleavage, not olivine). Granular texture, opx larger than cpx.
477653 *	2006aag 110	492488	7190726	Hornblendite, medium grained, probably metamorphic variety of originally opx-rich mafic-ultramafic intrusion.	
477654**	2006aag 112	492194	7190913	Amphibolite of presumed intrusive origin with disseminated sulphides. Silica content possibly increased by pre-metamorphic hydrothermal leaching.	Cpx >hbl - plag. Cpx and hbl layered. Minute qtz seams, disseminated opaques. Polished thin section.

*: Chemical analysis. **: Anomalous gold. Mineral abbreviations: Bt: biotite; cpx: clinopyroxene; crd: cordierite; ep: epidote; grt: garnet; mu: muscovite; opx: orthopyroxene; plag: plagioclase; pyrrh: pyrrhotite; qtz: quartz; rut: rutile; sill: sillimanite.

Appendix A (continued)

Sample	Loc.	Easting	Northing	Rock description	Thin section
477655**	2006aag 117	492509	7191469	Fine-grained, compositionally layered meta-andesite with disseminated iron sulphide. The lithology appears more than average siliceous (?hydrothermally leached). From the most conspicuous horizon 2-3 m thick.	Hbl - cpx - plag - qtz - ep (retrograde), disseminated opaques. Polished thin section.
477656*	2006aag 126	496584	7191568	Grey, fine-grained meta-andesite, indistinctly layered, with scattered pyrrhotite grains ?1 mm large.	
477657*	2006aag 134	495247	7191956	Meta-andesite, fine grained, indistinctly layered, with disseminated pyrrhotite grains ?1 mm large.	
477658*	2006aag 135	494164	7191727	Hornblendite of presumed intrusive origin in layered meta-andesite, medium grained, predating the granite (and deformation?).	Hbl, granular, rather weak colour, minor oxide exsolutions.
477659*	2006aag 136	493585	7190616	Sample for geochronology of an unusually felsic member of the meta-andesite, collected c. 30 m east of the large ultramafic body. The sample is fine-grained, contains plag-bt-qtz, and is indistinctly compositionally layered on a scale of centimetres.	Opx - hbl - bt - plag - qtz. Fine-grained.
477660**	2006aag 138	493572	7190730	Rusty weathering horizon 20 cm thick in ultramafic body, with medium-grained hbl-cpx, magnetite, and possibly opx or ol. No sulphides visible.	Opx - hbl - plag - minor disseminated opaques. Mm-scale layering, granular equilibrium texture. Polished thin section.
477661**	2006aag 138	493572	7190730	Opx-hornblende-layered ultramafic rock, strongly deformed, from the central part of the body.	
477662	2006aag 138	493572	7190730	Calcite vein and part of the diopsidic reaction rim.	
477663	2006aag 138	493572	7190730	Vein quartzite, with calcite-diopside margin.	
477664**	2006aag 139	493805	7190562	Dark grey meta-andesite, 1 mm-grained, layered on centimetre-scale, bt-?hbl-bearing, intermediate to mafic.	Hbl - cpx - plag >>qtz, ±granular. Hbl partially replaced by cpx in equilibrium (not retrograde texture).
477665*	2006aag 140	493871	7190546	Dark grey meta-andesite, 1 mm-grained, similar to that at loc. 139, adjacent to rusty weathering zone c. 5 m wide.	
477666*	2006aag 140	493871	7190546	Dark grey meta-andesite, fine grained, with pyrrhotite, disseminated and also seen along a hairline joint.	
477667*	2006aag 141	493543	7190201	Grey meta-andesite. Completely fresh, very homogeneous, finegrained, with barely recognisable compositional layering.	
477668*	2006aag 143	493774	7189845	Typical grey meta-andesite near the western margin of the eastern rusty weathering zone.	
477669**	2006aag 144	493721	7189893	Grey meta-andesite with disseminated pyrrhotite near the western rusty weathering zone.	Hbl - cpx - plag - pyrrh, equilibrium texture. Minute qtz seams.
477670*	2006aag 144	493721	7189893	Typical grey meta-andesite (without pyrrhotite) at the western margin of the same rusty weathering zone.	
477671	2006aag 156	493300	7190246	Very coarse-grained opx-mica rock from ultramafic body.	
477672	2006aag 156	493300	7190246	Diopsidic rock with carbonate veins (hand specimen only).	
477673*	2006aag 170	494518	7193079	Fine-rained, apparently almost completely homogeneous meta-andesite.	
477674**	2006aag 170	494518	7193079	Rusty weathering variety of fine-rained, apparently almost completely homogeneous meta-andesite, with disseminated ?pyrrhotite grains <1 mm in size.	Hbl - cpx - plag - pyrrh, equilibrium texture. Mafic appearance. Was quartz added by alteration?

*: chemical analysis. **: Anomalous gold. Mineral abbreviations: Bt: biotite; cpx: clinopyroxene; crd: cordierite; ep: epidote; grt: garnet; mu: muscovite; opx: orthopyroxene; plag: plagioclase; pyrrh: pyrrhotite; qtz: quartz; rut: rutile; sill: sillimanite.

Appendix A (continued)

Sample	Loc.	Easting	Northing	Rock description	Thin section
477675*	2006aag 173	493873	7192674	Dark grey, biotite-hornblende--bearing meta-andesite, locally layered on a 5 cm-scale, a little more mafic than most.	
477676*	2006aag 180	496290	7189175	Sillimanite-garnet-quartz-biotite-muscovite-cordierite rock, rusty weathering.	Grt - bt - sill - qtz - crd - mu - zircon (large grains, large halos in bt, probably high-U). Crd (confirm) is partially altered. Bt and mu much in sheaves. Sill mostly as fine fibrous aggregates.
477677*	2006aag 182	496207	7188904	Local met-andesite hostc. 35 m west of the sillimanite-garnet zone (here with minor hbl), 1 mm-grained, not migmatised, with minor diopside and very minor disseminated pyrrhotite.	
477678	2006aag 187	493663	7190870	Biotite orthogneiss, light grey, very homogeneous, medium grained. Representative for orthogneiss intruding the supracrustal rocks of the arc system.	Bt - hbl - plag - qtz. Minor retrogression, orthoamph. perhaps after minor px.
477679*	2006aag 199	492448	7190215	Medium-grained, homogeneous hornblende metagabbro, weakly deformed.	
Camp 2006-3, bay on eastern side of Qussuk					
477680**	2006aag 207	495442	7183200	Grey meta-andesite, fine grained, with unusually much very fine-grained pyrrhotite, apparently somewhat silicified (=leached?).	Grt - bt - sill - qtz - crd - zircon. Sill inclusions in crd and bt. Bt, crd and pyrrh in common, few mm thick veinlets.
477681*	2006aag 217	495824	7183364	Typical example of apparently strongly silicified (i.e., leached) meta-andesite with disseminated pyrrhotite.	
477682*	2006aag 231	495226	7178253	Meta-andesite with volcanic clasts, unmigmatised, no granite or pegmatite. Sample for zirconology, 2 bags.	Hbl - bt - plag - qtz - tit - zircon - opaque.
477683**	2006aag 234	495079	7178532	Meta-andesite with pyrrhotite mineralisation. Chips from several local blocks within 2 m across strike.	Bt - plag (partly altered) - qtz - ?pyrrh - ?oxide. Polished thin section.
477684*	2006aag 234	495079	7178532	Quartz vein within pyrrhotite-mineralised zone of meta-andesite.	Qtz - plag - ?pyrrh. Alternating qtz- and qtz-plag-rich zones. Millimetre-sized ?pyrrh patches. Polished thin section.
477685*	2006aag 236	495860	7180166	Sample of garnet-biotite-quartz-sulphide lens with possible sulphides inside garnet.	Grt - bt - plag - qtz - hbl (spongy, blue-green). In part retrogressive texture. Polished thin section.
477686**	2006aag 242	495860	7180166	Garnet-biotite-quartz -(pyrite-pyrrhotite) rock, from the alteration zone under the big hammer (photo 282).	Grt - bt - qtz - zircon - ?pyrrh. Grt poikiloblastic, ?1 cm. ?Rut needles in qtz. No plag or crd. Polished thin section.
477687*	2006aag 242	495860	7180166	Mafic metatuff (the photographed locality).	Hbl - plag - bt (very minor). Fresh, equilibrium texture. Hbl has pale sectors with lamellar twins.
477688*	2006aag 242	495860	7180166	Adjacent (hanging wall) andesitic metatuff.	Bt - qtz- plag - ap. Bt finely dispersed.
Ivisaat mountain, sampled during excursion					
477689	2006aag 249	495090	7184676	Hydrothermally altered and metamorphosed rock with blackish grey garnets and blue quartz, from the garnet-rich zone at Ivisaat.	Grt - bt - qtz - crd - zircon - ?pyrrh. Grt poikiloblastic with qtz and oaque inclusions. Crd has rims packed with very fine-grained sill needles.
Camp 2006-4, inland camp on peninsula east of Qussuk					
477690	2006aag 257	494067	7171276	Siliceous, fine- to medium-grained quartz-garnet-magnetite-?biotite rock with minor Fe sulphides. Presumably hydrothermally altered.	Qtz - Kfsp - bt - grt -ep (secondary alteration of biotite). Grt poikiloblastic. The paragenesis might suggest an S-type granite, but the texture is granular, not granitic.
477691*	2006aag 283	494340	7172128	Meta-andesite, fine-grained and strongly deformed. Collected 15 m SW of loc. 283, ?unaltered host to mineralised sample 477692.	Bt - hbl - plag - qtz - ep - zircon -carb (very minor, interstitial). No opaques.

*: chemical analysis. **: Anomalous gold. Mineral abbreviations: Bt: biotite; cpx: clinopyroxene; crd: cordierite; ep: epidote; grt: garnet; mu: muscovite; opx: orthopyroxene; plag: plagioclase; pyrrh: pyrrhotite; qtz: quartz; rut: rutile; sill: sillimanite.

Appendix A (continued)

Sample	Loc.	Easting	Northing	Rock description	Thin section
477692**	2006aag 283	494340	7172128	Fine-grained, rusty weathering meta-andesite from the central part of the mineralised zone, with hairline rusty weathering seams. The lithology appears more siliceous than 477691 and 477693 (leached).	Bt - qtz - albite (? Or possibly crd, partially altered) - ep (alteration of hbl) - pyrrh (disseminated). Bt dark. Secondary retrogression with ep masses after hbl. Polished thin section.
477693*	2006aag 283	494340	7172128	25 m NE of loc. 283, the apparently unaltered host meta-andesite, fine grained, darker (more mafic) than 477691.	Hbl >bt - plag >qtz - ap - ?pyrrh (disseminated). Equilibrium texture.
477694*	2006aag 244b	494320	7175762	Fine-grained meta-andesite with disseminated iron sulphides.	
477695**	2006aag 244c	494746	7176149	Fine-grained meta-andesite with disseminated iron sulphides.	
477696*	2006aag 286	494113	7171119	Central, bleached part of hydrothermal alteration zone. Quartz, ?plagioclase, minor muscovite, garnet, and in places biotite. Did not find sillimanite.	Bt - sill - qtz - ?crd - mu (minor) - zircon (plenty). Sill as masses of very fine needles (?andalusite pseudomorphs). ?Crd with bt and grt, not with qtz, and rare lamellar twins, point away from plag.
477697*	2006aag 294	493482	7171399	Meta-andesite with disseminated to semi-massive iron sulphide.	
Camp 2006-5, inland camp on Bjørneøen					
488801*	2006aag 300	488047	7144140	Quartz-plagioclase-biotite-epidote-(Fe-sulphide) rock, fine grained, finely layered (?tectonically), from the central part of the sulphide mineralised zone. Felsic metatuff (not hydrothermally altered?)	Bt - ep - plag - qtz. Very fine-grained, layered, ep well crystallised and in equilibrium with other silicates.
488802**	2006aag 300	488047	7144140	Very fine-grained, indistinctly layered amphi-bolite, typical of the rocks surrounding the mineralised zone.	Hbl - plag. Very fine-grained, mafic, mostly hbl.
488103	2006aag 313	485785	7146073	Volcaniclastic meta-andesite.	Hbl - plag - qtz - ep - carb - tit. Fine-grained, low meta-morphic grade. Ep secondary (minor retrogression).
488104	2006aag 321	488229	7144601	Display piece, mafic metatuff.	
488105	2006aag 322	488346	7144636	Felsic metasedimentary rock, representative of the outcrop.	Qtz - plag - bt - mu - ep. Mm-scale layered, very fine-grained, except ?late, poikiloblastic mu.
488106	2006aag 322	488346	7144636	Metavolcanic rock with centimetre-sized felsic clasts. Possibly a lapilli tuff.	Bt - plag - qtz. Plag ggregates ?1 cm in size mostly consist of few, relatively large crystals with different orientations, zoning, and large single ?Carlsbad twins (possibly igneous). The thin section thus supports an interpretation as lapilli tuff.
488107	2006aag 323	488436	7144668	Volcaniclastic rock with concave clast shapes interpreted as fiammes, from fold hinge.	
488108	2006aag 325	488553	7144739	Sample of fine-grained intrusive tonalite sheet 30 cm thick, for geochronology.	Plag - qtz - hbl - ap. Fine-grained.

*: chemical analysis. **: Anomalous gold. Mineral abbreviations: Ap: apatite; bt: biotite; cpx: clinopyroxene; crd: cordierite; ep: epidote; grt: garnet; mu: muscovite; opx: orthopyroxene; plag: plagioclase; pyrrh: pyrrhotite; qtz: quartz; rut: rutile; sill: sillimanite.

APPENDIX B. – Major and ‘exploration grade’ trace element analyses

Appendix B. Major and 'exploration grade' trace element analyses

Element	SiO2	Al_2O_3	Fe_2O_3(T)	MnO	MgO	CaO	Na_2O	K_2O	TiO_2	P_2O_5	LOI	Total
Conc.	%	%	%	%	%	%	%	%	%	%	%	%
Det. lim.	0.01	0.01	0.01	0.01	0.01	0.01	0.01	0.01	0.01	0.01	0.01	0.01
Method*	F	F	F	F	F	F	F	F	F	F	F	F
477621	46.70	14.76	12.59	0.21	8.63	12.34	1.68	0.38	0.60	0.06	0.83	98.79
477622	58.22	15.77	8.17	0.12	3.24	6.57	3.46	1.26	0.88	0.27	0.65	98.61
477623	57.11	14.53	9.62	0.69	5.14	7.23	0.55	1.95	0.64	0.16	2.01	99.64
477624	56.49	14.31	7.74	0.49	6.72	4.23	1.31	2.70	0.67	0.19	4.11	98.95
477625	55.27	14.35	17.59	0.36	6.56	0.51	0.36	1.68	1.27	0.04	1.20	99.17
477627	68.34	13.58	11.05	0.31	2.69	0.37	0.28	1.80	0.58	0.16	0.28	99.44
477629	57.24	15.37	8.72	0.15	4.55	7.02	3.01	1.09	0.72	0.15	0.78	98.79
477630	78.95	16.06	0.64	< 0.01	0.20	0.15	0.41	1.14	0.80	0.07	0.66	99.09
477631	62.84	14.59	6.16	0.14	4.37	5.76	2.33	1.49	0.58	0.14	0.80	99.19
477632	64.69	14.69	7.23	0.32	3.74	6.78	1.19	0.55	0.59	0.13	0.37	100.30
477633	60.25	16.20	6.51	0.20	4.64	6.75	1.12	1.58	0.52	0.11	1.32	99.17
477634	63.21	15.44	6.45	0.30	3.97	6.51	1.87	0.34	0.62	0.15	0.83	99.67
477635	76.65	18.21	2.59	0.02	0.17	0.32	0.25	0.39	0.81	0.13	1.00	100.50
477636	62.38	15.07	6.51	0.43	5.31	5.45	1.15	1.76	0.62	0.14	1.37	100.20
477637	55.93	16.01	14.92	0.53	6.39	1.38	0.63	2.00	0.95	0.14	0.13	99.01
477638	57.51	16.54	10.65	0.45	4.71	4.90	0.84	2.24	0.94	0.22	0.51	99.52
477639	58.02	15.72	13.84	0.45	6.03	1.51	0.63	2.03	1.10	0.16	0.22	99.70
477640	47.31	13.34	13.01	0.33	9.97	11.06	1.17	0.74	1.28	0.20	1.14	99.55
477641	67.64	14.24	6.95	0.16	2.72	1.84	1.99	2.61	0.29	0.08	1.03	99.53
477642	61.81	14.47	13.82	0.29	4.74	0.55	0.57	2.23	0.62	0.08	0.60	99.78
477643	64.89	15.05	5.32	0.17	3.83	6.07	0.78	1.99	0.57	0.14	0.78	99.59
477644	59.06	14.07	15.25	0.14	5.16	0.46	0.68	3.12	0.62	0.06	0.51	99.12
477645	52.50	16.37	10.44	0.17	5.14	6.80	3.86	1.27	1.17	0.16	1.96	99.83
477646	54.55	17.80	10.31	0.16	2.84	7.75	3.60	1.00	0.80	0.26	0.61	99.67
477647	59.61	13.40	9.73	0.12	3.45	7.50	2.41	0.75	0.49	0.04	1.60	99.10
477651	54.08	17.81	7.04	0.17	2.63	12.87	3.16	0.46	0.72	0.13	0.67	99.74
477652	48.50	8.11	12.33	0.16	21.44	7.28	0.80	0.18	0.30	0.04	0.96	100.10
477653	47.39	15.13	11.89	0.18	8.31	9.81	2.61	0.93	1.00	0.17	1.31	98.73
477654	48.10	12.65	17.84	0.33	3.57	9.82	2.91	0.50	2.59	0.32	0.20	98.83
477655	54.65	13.83	9.83	0.14	5.28	9.31	1.99	0.42	0.54	0.03	2.75	98.78
477656	50.19	15.35	11.66	0.26	2.41	16.21	2.20	0.18	1.03	0.09	0.20	99.79
477657	58.68	10.28	10.02	0.17	5.67	9.84	2.12	0.41	0.42	0.02	1.40	99.04
477658	46.69	10.23	11.90	0.20	16.03	10.69	1.51	0.31	0.45	0.03	1.66	99.70
477659	62.53	16.76	4.92	0.04	3.00	6.03	3.95	0.81	0.52	0.10	0.32	98.99
477660	49.13	4.22	27.82	0.27	8.28	7.57	0.94	0.22	0.23	< 0.01	0.19	98.88
477661	46.58	7.99	11.01	0.13	22.20	8.40	0.68	0.04	0.30	0.03	1.60	98.95
477664	50.44	13.72	10.29	0.13	6.86	12.40	2.82	0.66	1.05	0.08	0.28	98.73
477665	54.59	16.28	8.95	0.13	4.35	7.17	3.37	1.67	1.06	0.54	0.88	98.99
477666	54.82	15.05	9.41	0.12	5.71	8.56	3.31	0.85	0.83	0.14	0.91	99.72
477667	54.01	15.87	10.12	0.09	5.34	9.20	3.23	0.81	0.91	0.12	0.34	100.10
477668	50.41	14.91	10.45	0.16	6.64	8.48	3.30	1.51	1.23	0.69	1.18	98.95
477669	54.32	15.07	7.34	0.14	7.19	10.70	2.84	0.47	0.64	0.13	1.42	100.30
477670	54.51	16.84	8.93	0.13	4.65	7.90	3.35	1.47	1.01	0.52	1.03	100.40
477673	55.56	13.75	7.92	0.16	7.32	10.73	1.84	0.19	0.58	0.10	0.79	98.95
477674	54.55	13.39	8.10	0.17	7.41	11.38	2.63	0.39	0.57	0.24	1.07	99.91
477675	50.63	14.24	10.31	0.18	8.10	11.33	2.37	0.49	0.58	0.05	0.69	98.98
477676	64.88	12.91	10.74	0.35	3.97	0.37	0.71	3.14	0.77	0.08	1.63	99.56
477677	59.15	14.87	7.09	0.11	3.99	7.62	3.04	1.33	0.65	0.17	0.56	98.58
477679	49.03	14.90	11.02	0.18	7.22	12.21	2.01	0.42	0.90	0.15	0.97	98.99
477680	70.57	11.98	6.98	0.04	3.21	1.31	1.09	1.05	0.65	0.02	2.42	99.33
477681	73.44	11.33	6.04	0.08	1.31	2.08	2.58	0.84	0.29	0.02	1.50	99.51
477682	62.52	14.87	7.15	0.13	3.32	5.37	3.11	1.62	0.80	0.16	0.85	99.89
477683	55.01	11.40	17.68	0.01	2.00	2.31	2.55	1.40	0.69	< 0.01	7.87	100.30
477684	84.11	7.86	2.02	< 0.01	0.21	2.10	2.16	0.23	0.07	0.01	0.80	99.58
477685	53.41	12.97	14.29	0.15	6.90	3.65	1.25	3.31	0.82	0.10	1.91	98.76
477686	53.26	13.45	22.93	0.15	5.52	1.17	0.60	2.37	0.79	0.04	0.11	100.40
477687	48.15	15.43	12.32	0.20	9.81	10.19	2.01	0.52	0.67	0.05	0.97	100.30
477688	71.46	13.71	3.77	0.02	2.21	2.55	3.43	1.77	0.54	0.09	0.69	100.30
477691	58.15	14.28	7.70	0.13	5.00	4.91	2.67	3.00	0.65	0.12	2.25	98.87
477692	61.50	14.63	10.44	0.08	2.98	2.07	3.40	2.31	0.75	0.14	2.04	100.30
477693	58.04	14.15	12.13	0.16	3.10	6.67	3.49	0.58	1.21	0.20	0.41	100.10
477694	66.51	14.07	6.18	0.03	2.66	4.29	2.34	1.58	0.74	0.21	1.18	99.79
477695	58.76	15.32	10.44	0.12	3.12	4.61	3.45	1.93	1.05	0.17	1.56	100.50
477696	73.60	11.17	6.04	0.10	2.47	1.35	1.96	2.13	0.36	0.04	0.94	100.20
477697	57.53	10.17	10.60	0.16	4.53	8.60	2.51	0.36	0.36	< 0.01	3.99	98.82
488101	70.80	16.07	2.68	0.04	1.24	3.57	3.31	1.27	0.25	0.09	0.69	100.00
488102	50.52	13.91	13.68	0.20	6.76	10.67	1.81	0.28	1.26	0.15	1.04	100.30

*Method: F = Fusion inductively coupled plasma mass spectrometry (ICP-MS).

Appendix B. Major and 'exploration grade' trace element analyses (continued)

Element	Cu	Sc	U	Ce	Nd	Sm	Au	Ag	As	Ba	Be	Bi	Cd	Co	Cr	Cs	Hf	Ir	Mo	Ni
Conc.	ppm	ppm	ppm	ppm	ppm	ppm	ppb	ppm	ppm	ppm	ppm	ppm	ppm	ppm	ppm	ppm	ppm	ppb	ppm	ppm
Det. lim.	1	0.1	0.5	3	5	0.1	5	0.5	2	3	1	2	0.5	1	1	0.5	0.5	5	5	1
Method*	T	I	I	I	I	I	I	M	I	M	F	T	T	I	I	I	I	I	I	T
477621	69	45.3	< 0.5	9	< 5	1.5	< 5	< 0.5	< 2	61	< 1	14	< 0.5	55	287	< 0.5	< 0.5	< 5	< 5	159
477622	33	23.1	< 0.5	29	19	3.3	< 5	< 0.5	< 2	389	1	6	< 0.5	24	38	< 0.5	2.8	< 5	< 5	33
477623	29	22.1	0.9	38	15	3.5	9	< 0.5	< 2	678	1	8	< 0.5	28	290	< 0.5	3.1	< 5	< 5	117
477624	68	24.6	1.4	35	15	3.4	23	0.6	< 2	1420	1	9	0.6	25	346	1.7	3.0	< 5	< 5	25
477625	177	30.9	< 0.5	42	16	3.2	34	< 0.5	< 2	505	4	6	0.5	35	< 1	< 0.5	5.0	< 5	< 5	30
477627	17	17.0	2.8	74	27	7.7	< 5	< 0.5	< 2	241	< 1	< 2	1.0	9	5	< 0.5	9.3	< 5	< 5	10
477629	22	26.4	< 0.5	29	16	3.0	7	< 0.5	< 2	382	1	7	< 0.5	26	66	< 0.5	2.5	< 5	< 5	37
477630	9	8.4	1.9	67	23	5.2	< 5	0.5	< 2	673	< 1	< 2	< 0.5	< 1	14	< 0.5	6.2	< 5	< 5	2
477631	30	15.6	< 0.5	37	16	3.2	< 5	0.8	< 2	485	1	6	< 0.5	25	186	1.0	3.4	< 5	< 5	94
477632	40	19.0	1.0	32	13	2.7	14	0.6	< 2	347	1	8	< 0.5	17	219	< 0.5	3.0	< 5	< 5	60
477633	34	21.8	< 0.5	26	9	2.3	10	0.7	< 2	366	1	12	0.5	44	243	< 0.5	2.2	< 5	< 5	156
477634	70	19.5	< 0.5	39	11	3.5	< 5	0.7	< 2	178	< 1	9	< 0.5	11	205	< 0.5	3.0	< 5	< 5	66
477635	72	9.7	< 0.5	29	10	2.3	18	0.6	< 2	286	< 1	< 2	< 0.5	9	215	< 0.5	4.0	< 5	< 5	71
477636	20	17.4	1.4	38	13	3.2	8	0.6	< 2	346	1	7	0.6	14	145	< 0.5	3.3	< 5	< 5	48
477637	28	32.4	1.1	29	13	3.2	< 5	< 0.5	< 2	425	2	5	< 0.5	25	68	2.4	3.1	< 5	< 5	42
477638	58	26.6	1.0	30	14	3.6	16	< 0.5	< 2	581	1	9	< 0.5	25	26	1.7	3.1	< 5	< 5	39
477639	92	26.2	< 0.5	34	15	3.8	12	< 0.5	< 2	389	3	7	< 0.5	25	109	1.6	3.9	< 5	< 5	44
477640	11	23.4	< 0.5	34	16	4.4	< 5	< 0.5	< 2	202	2	17	< 0.5	58	562	< 0.5	2.2	< 5	< 5	292
477641	32	10.0	1.3	55	22	5.2	< 5	1.1	< 2	579	1	3	< 0.5	10	6	2.6	6.6	< 5	< 5	13
477642	116	14.9	1.5	41	14	3.4	39	0.6	< 2	540	1	3	3.0	20	129	1.6	3.0	< 5	< 5	76
477643	7	13.8	1.8	37	10	3.1	< 5	< 0.5	< 2	768	1	4	< 0.5	21	104	< 0.5	3.4	< 5	< 5	75
477644	45	15.1	< 0.5	40	12	3.3	34	< 0.5	< 2	602	1	4	0.5	18	162	1.2	3.7	< 5	< 5	62
477645	58	35.3	0.9	26	12	4.0	< 5	< 0.5	< 2	251	2	6	< 0.5	41	261	< 0.5	2.7	< 5	< 5	74
477646	18	13.9	< 0.5	51	21	5.5	< 5	< 0.5	< 2	155	1	5	< 0.5	25	9	1.9	2.8	< 5	< 5	7
477647	168	38.3	< 0.5	7	< 5	1.2	< 5	0.6	< 2	112	1	7	< 0.5	17	311	< 0.5	< 0.5	< 5	16	38
477651	21	28.8	< 0.5	34	16	3.3	< 5	< 0.5	< 2	157	1	8	< 0.5	32	32	< 0.5	2.1	< 5	< 5	41
477652	10	26.9	< 0.5	< 3	< 5	0.7	14	< 0.5	< 2	18	< 1	30	< 0.5	77	2010	< 0.5	0.7	< 5	< 5	620
477653	22	32.8	< 0.5	9	< 5	1.9	< 5	< 0.5	< 2	122	< 1	15	< 0.5	47	343	2.4	0.9	< 5	< 5	170
477654	52	19.6	< 0.5	37	18	6.6	10	< 0.5	< 2	160	2	5	< 0.5	23	8	< 0.5	3.5	< 5	< 5	13
477655	196	42.4	< 0.5	17	7	1.6	48	< 0.5	< 2	101	2	10	< 0.5	47	652	< 0.5	1.3	< 5	< 5	230
477656	107	43.5	< 0.5	10	< 5	2.6	7	< 0.5	< 2	85	1	11	< 0.5	50	105	< 0.5	1.7	< 5	< 5	82
477657	87	30.1	< 0.5	5	< 5	1.0	< 5	< 0.5	< 2	147	< 1	12	< 0.5	71	1390	< 0.5	< 0.5	< 5	< 5	461
477658	34	58.1	1.1	5	< 5	0.9	9	< 0.5	< 2	40	< 1	22	< 0.5	99	3980	< 0.5	< 0.5	< 5	< 5	513
477659	5	14.1	1.5	23	8	2.2	6	< 0.5	< 2	354	1	4	< 0.5	22	29	< 0.5	2.2	< 5	< 5	17
477660	538	19.5	< 0.5	7	< 5	0.7	87	< 0.5	< 2	113	1	13	< 0.5	67	1220	< 0.5	< 0.5	< 5	6	343
477661	9	28.1	1.6	< 3	< 5	0.7	29	< 0.5	< 2	17	< 1	35	< 0.5	91	3920	< 0.5	< 0.5	< 5	< 5	1050
477664	14	37.3	1.5	11	7	2.4	15	< 0.5	< 2	118	1	10	< 0.5	32	129	< 0.5	1.5	< 5	< 5	125
477665	9	18.6	3.0	107	49	7.7	< 5	< 0.5	< 2	774	1	7	< 0.5	29	29	1.5	2.9	< 5	< 5	51
477666	45	24.3	7.1	23	9	2.7	< 5	< 0.5	< 2	210	1	10	< 0.5	32	161	< 0.5	2.4	< 5	< 5	88
477667	24	29.3	2.8	24	11	2.8	< 5	< 0.5	< 2	285	1	9	< 0.5	32	76	< 0.5	2.6	< 5	< 5	26
477668	59	21.6	2.4	93	48	7.4	< 5	< 0.5	< 2	490	1	7	< 0.5	38	183	< 0.5	2.8	< 5	< 5	139
477669	60	46.0	0.8	10	5	1.4	12	< 0.5	< 2	96	< 1	9	< 0.5	51	380	1.3	1.0	< 5	< 5	97
477670	16	18.6	1.3	88	42	7.1	< 5	< 0.5	5	790	1	7	< 0.5	31	20	1.2	2.7	< 5	< 5	49
477673	7	46.0	< 0.5	5	< 5	1.3	< 5	< 0.5	< 2	32	1	10	< 0.5	55	399	< 0.5	1.1	< 5	< 5	132
477674	47	47.2	< 0.5	8	< 5	1.4	20	< 0.5	< 2	60	1	12	< 0.5	17	485	< 0.5	< 0.5	< 5	< 5	26
477675	17	46.7	< 0.5	7	< 5	1.5	< 5	< 0.5	< 2	56	1	12	< 0.5	56	511	< 0.5	0.9	< 5	< 5	180
477676	23	18.3	1.4	110	40	10.4	< 5	1.6	< 2	454	< 1	< 2	< 0.5	15	2	2.0	12.2	< 5	< 5	4
477677	15	40.8	< 0.5	7	< 5	1.8	< 5	< 0.5	2	515	2	8	< 0.5	43	443	< 0.5	1.1	< 5	< 5	46
477679	55	41.2	< 0.5	6	5	1.7	< 5	< 0.5	< 2	45	< 1	10	< 0.5	42	426	< 0.5	1.1	< 5	< 5	91
477680	253	12.3	0.9	84	44	6.9	27	< 0.5	< 2	871	< 1	4	< 0.5	9	12	< 0.5	11.1	< 5	< 5	3
477681	129	7.3	< 0.5	80	51	6.2	13	< 0.5	< 2	783	< 1	< 2	0.5	3	< 1	< 0.5	9.5	< 5	< 5	2
477682	81	20.6	< 0.5	29	15	2.8	< 5	< 0.5	< 2	473	1	2	< 0.5	20	36	1.4	4.2	< 5	< 5	32
477683	735	6.5	< 0.5	44	24	4.1	74	< 0.5	< 2	555	1	6	< 0.5	49	22	< 0.5	5.4	< 5	< 5	184
477684	39	1.4	< 0.5	41	23	2.6	15	< 0.5	< 2	116	< 1	< 2	< 0.5	3	8	< 0.5	12.3	< 5	< 5	3
477685	197	23.5	< 0.5	23	14	2.1	15	< 0.5	< 2	320	1	7	< 0.5	33	259	7.3	3.0	< 5	< 5	107
477686	925	24.1	< 0.5	37	21	3.1	99	< 0.5	< 2	653	< 1	8	< 0.5	53	324	2.5	6.5	< 5	< 5	170
477687	50	45.0	< 0.5	9	< 5	1.5	< 5	< 0.5	< 2	48	< 1	10	< 0.5	48	349	< 0.5	1.2	< 5	< 5	151
477688	7	9.9	1.9	56	35	4.5	< 5	< 0.5	< 2	552	1	< 2	< 0.5	9	< 1	2.5	7.6	< 5	< 5	2
477691	7	19.0	< 0.5	27	20	2.9	14	< 0.5	< 2	470	1	6	< 0.5	31	378	3.7	3.4	< 5	< 5	137
477692	580	18.4	< 0.5	29	17	2.7	38	1.2	< 2	264	1	4	< 0.5	14	71	2.2	5.0	< 5	< 5	12
477693	68	30.9	< 0.5	27	16	3.3	17	< 0.5	< 2	120	2	2	< 0.5	33	43	< 0.5	3.6	< 5	< 5	33
477694	46	14.3	0.9	22	12	1.5	< 5	< 0.5	< 2	1050	1	< 2	< 0.5	11	82	1.7	4.3	< 5	< 5	21
477695	143	19.7	1.4	20	14	2.8	32	< 0.5	< 2	821	1	2	< 0.5	19	79	9.4	4.3	< 5	< 5	31
477696	21	9.9	1.6	57	39	5.3	< 5	< 0.5	< 2	485	1	2	0.6	7	10	< 0.5	9.1	< 5	< 5	4
477697	258	41.3	1.3	< 3	< 5	0.7	< 5	< 0.5	< 2	107	< 1	4	< 0.5	69	2620	< 0.5	1.0	< 5	< 5	789
488101	11	2.4	1.2	21	10	1.2	6	< 0.5	< 2	416	< 1	< 2	< 0.5	3	8	5.1	2.8	< 5	< 5	5
488102	71	45.6	< 0.5	11	11	2.2	30	< 0.5	< 2	120	1	7	< 0.5	47	284	< 0.5	1.8	< 5	< 5	63

*Methods: F = fusion inductively coupled plasma mass spectrometry (ICP-MS); I = instrumental neutron activation analysis (INNA); M = Multi INNA/'total' four-acid digestion-ICP; T = 'total' four-acid digestion-ICP.

Appendix B. Major and 'exploration grade' trace element analyses (continued)

Element	Pb	Rb	S	Sb	Sr	Ta	Th	V	W	Y	Zn	Zr	La	Eu	Tb	Yb	Lu	Mass
Conc.	ppm	ppm	%	ppm	ppm	ppm	ppm	ppm	ppm	ppm	ppm	ppm	ppm	ppm	ppm	ppm	ppm	g
Det. lim.	5	20	0.001	0.2	2	1	0.5	5	3	1	1	2	0.2	0.1	0.5	0.1	0.05	
Method*	T	I	T	I	F	I	I	F	I	F	T	F	I	I	I	I	I	I
477621	11	< 20	0.075	< 0.2	93	< 1	< 0.5	251	< 3	18	97	32	2.3	0.5	< 0.5	2.3	0.34	1.484
477622	16	< 20	0.025	< 0.2	292	< 1	2.2	173	< 3	15	89	124	16.9	1.0	< 0.5	1.3	0.28	1.389
477623	21	60	0.460	0.3	139	< 1	3.1	126	< 3	14	415	135	21.1	1.0	< 0.5	1.4	0.26	1.445
477624	29	60	2.080	< 0.2	75	< 1	3.3	141	< 3	18	477	126	19.0	1.1	< 0.5	2.1	0.34	1.410
477625	< 5	80	0.964	< 0.2	4	< 1	4.8	251	< 3	42	346	211	23.0	0.7	1.0	3.5	0.59	1.571
477627	16	60	0.015	< 0.2	6	2	8.3	42	< 3	57	257	410	40.8	1.6	1.3	5.6	0.85	1.417
477629	18	< 20	0.028	< 0.2	299	< 1	2.1	196	< 3	17	83	115	15.2	0.9	< 0.5	1.5	0.28	1.555
477630	10	< 20	0.003	< 0.2	45	< 1	8.6	62	9	20	7	265	38.5	1.1	0.8	1.8	0.34	1.526
477631	17	70	0.086	< 0.2	170	< 1	3.6	110	< 3	12	79	152	20.5	0.8	< 0.5	1.0	0.20	1.505
477632	26	< 20	0.166	< 0.2	248	< 1	4.1	124	< 3	14	98	127	20.7	0.8	< 0.5	1.4	0.25	1.463
477633	58	70	0.955	< 0.2	208	< 1	3.7	143	< 3	11	373	99	16.2	0.7	< 0.5	0.9	0.20	1.215
477634	28	50	0.504	< 0.2	181	1	4.4	124	< 3	16	216	144	22.2	0.9	< 0.5	1.3	0.28	1.553
477635	10	< 20	1.380	< 0.2	59	< 1	4.0	124	4	16	25	170	17.1	0.9	< 0.5	1.0	0.19	1.222
477636	43	< 20	0.301	< 0.2	92	1	4.5	107	< 3	17	367	150	19.8	0.7	< 0.5	1.6	0.27	1.243
477637	< 5	70	0.013	< 0.2	37	< 1	3.5	183	< 3	27	116	140	16.4	0.8	0.8	2.4	0.35	1.859
477638	21	40	0.178	< 0.2	101	< 1	2.4	167	3	22	152	147	16.2	1.2	0.7	2.0	0.32	1.413
477639	9	40	0.109	< 0.2	24	< 1	4.0	227	5	26	437	176	18.3	0.9	0.5	2.4	0.39	1.784
477640	6	< 20	0.035	< 0.2	109	< 1	0.9	173	7	18	107	118	16.6	1.3	< 0.5	1.3	0.24	1.693
477641	12	110	0.100	< 0.2	67	2	6.4	10	5	35	70	291	29.9	1.5	< 0.5	3.3	0.51	1.469
477642	10	40	0.412	< 0.2	53	< 1	5.2	105	< 3	15	555	159	22.7	0.8	< 0.5	1.4	0.19	1.477
477643	44	50	0.024	< 0.2	168	< 1	4.8	94	6	14	103	148	21.1	0.9	< 0.5	1.0	0.21	1.481
477644	7	100	0.123	< 0.2	52	< 1	4.6	107	4	14	137	153	22.2	0.9	0.5	1.1	0.22	1.642
477645	13	60	0.034	< 0.2	222	< 1	0.9	226	6	23	134	105	13.0	1.3	0.7	2.0	0.36	1.345
477646	17	< 20	0.030	< 0.2	331	< 1	2.6	80	5	28	106	153	24.6	1.6	< 0.5	2.8	0.49	1.390
477647	18	< 20	0.259	< 0.2	77	< 1	1.0	230	8	16	84	28	2.1	0.5	0.6	1.9	0.27	1.481
477651	16	< 20	0.049	< 0.2	178	< 1	1.8	178	< 3	21	79	84	14.8	1.1	0.6	2.1	0.37	1.681
477652	< 5	20	0.038	< 0.2	30	< 1	< 0.5	141	5	8	27	15	1.0	0.3	< 0.5	0.9	0.16	1.695
477653	10	50	0.060	< 0.2	142	< 1	< 0.5	233	3	17	85	52	3.2	1.0	< 0.5	1.8	0.27	1.727
477654	15	< 20	0.058	< 0.2	381	< 1	< 0.5	289	< 3	29	140	149	15.7	2.1	0.8	2.1	0.31	1.763
477655	12	< 20	1.680	< 0.2	166	< 1	< 0.5	235	4	11	106	47	7.1	0.6	< 0.5	1.2	0.19	1.608
477656	18	< 20	0.133	< 0.2	141	< 1	1.2	288	< 3	30	98	55	4.3	0.9	0.7	3.3	0.57	1.379
477657	< 5	< 20	0.712	< 0.2	76	< 1	< 0.5	222	< 3	10	107	15	1.5	< 0.1	< 0.5	1.0	0.16	1.716
477658	< 5	< 20	0.087	< 0.2	23	< 1	< 0.5	188	< 3	10	73	21	1.5	0.4	< 0.5	1.2	0.19	1.513
477659	11	< 20	0.019	< 0.2	312	< 1	2.2	106	6	13	12	101	12.4	0.7	< 0.5	1.1	0.21	1.603
477660	< 5	< 20	1.690	< 0.2	39	< 1	< 0.5	110	74	6	40	9	2.4	< 0.1	< 0.5	0.6	0.09	1.697
477661	< 5	< 20	0.043	< 0.2	19	< 1	0.6	131	< 3	7	34	17	1.2	0.4	< 0.5	0.9	0.14	1.356
477664	13	< 20	0.050	< 0.2	292	< 1	0.7	298	< 3	18	32	55	4.8	0.9	< 0.5	1.5	0.24	1.574
477665	16	60	0.056	< 0.2	677	< 1	5.7	175	< 3	18	92	135	57.5	2.1	< 0.5	1.3	0.28	1.314
477666	12	50	0.440	< 0.2	277	< 1	1.9	188	< 3	17	63	106	12.4	1.0	< 0.5	1.4	0.21	1.327
477667	11	< 20	0.049	< 0.2	421	< 1	1.9	240	3	17	25	99	11.5	1.0	0.5	1.5	0.25	1.607
477668	14	80	0.318	< 0.2	667	< 1	2.8	199	< 3	18	99	148	50.1	2.2	< 0.5	1.4	0.24	1.352
477669	8	< 20	0.701	< 0.2	92	< 1	0.7	285	< 3	11	58	40	3.3	< 0.1	< 0.5	1.2	0.16	1.555
477670	14	< 20	0.257	< 0.2	822	< 1	4.2	171	< 3	16	85	122	45.3	2.0	< 0.5	1.2	0.21	1.409
477673	12	< 20	0.040	< 0.2	87	< 1	0.6	241	< 3	11	62	34	2.8	0.6	< 0.5	1.0	0.17	1.494
477674	13	< 20	0.083	< 0.2	89	< 1	< 0.5	264	< 3	11	80	36	2.6	0.5	< 0.5	1.3	0.23	1.305
477675	12	30	0.045	< 0.2	145	< 1	< 0.5	255	< 3	12	64	27	2.8	0.6	< 0.5	1.5	0.24	1.714
477676	15	100	0.105	< 0.2	29	< 1	13.8	35	< 3	57	200	505	59.8	1.5	1.6	6.7	1.02	1.625
477677	16	< 20	0.037	0.2	241	< 1	< 0.5	144	< 3	14	93	107	3.2	0.7	< 0.5	1.4	0.26	1.415
477679	13	< 20	0.073	< 0.2	115	< 1	0.6	235	< 3	15	81	44	2.8	0.9	< 0.5	1.4	0.24	1.768
477680	< 5	40	1.610	< 0.2	181	1	10.1	6	< 3	27	30	440	51.4	2.2	0.5	2.3	0.35	1.040
477681	5	< 20	1.130	< 0.2	91	< 1	7.7	< 5	< 3	58	197	377	41.0	1.7	1.1	5.9	0.86	1.274
477682	< 5	40	0.036	< 0.2	173	< 1	2.0	185	< 3	16	43	137	18.1	1.1	< 0.5	1.7	0.22	1.333
477683	12	< 20	8.640	< 0.2	60	< 1	7.1	43	10	31	26	215	26.9	1.2	0.7	2.6	0.39	1.350
477684	5	< 20	0.412	< 0.2	121	< 1	6.2	< 5	< 3	8	7	441	26.4	0.9	< 0.5	0.9	0.14	1.156
477685	11	130	1.130	< 0.2	101	< 1	2.6	164	< 3	14	125	128	13.5	1.1	< 0.5	1.6	0.21	1.467
477686	< 5	60	0.634	< 0.2	81	< 1	4.5	145	< 3	25	55	248	23.0	1.3	0.8	2.6	0.41	1.509
477687	6	< 20	0.063	< 0.2	88	< 1	< 0.5	271	< 3	22	72	39	3.1	0.7	< 0.5	2.6	0.39	1.275
477688	< 5	< 20	0.002	< 0.2	159	< 1	6.8	11	< 3	27	14	296	35.8	1.2	0.5	2.6	0.35	1.166
477691	10	90	0.002	< 0.2	300	< 1	3.8	120	< 3	16	118	139	17.4	1.1	< 0.5	1.6	0.27	1.163
477692	7	70	0.314	< 0.2	182	< 1	4.2	129	< 3	21	60	191	19.2	0.9	< 0.5	2.2	0.33	1.205
477693	10	< 20	0.048	< 0.2	189	< 1	3.6	242	< 3	28	101	131	16.0	1.2	< 0.5	3.0	0.48	1.252
477694	< 5	60	0.066	< 0.2	133	< 1	6.2	98	< 3	7	17	151	14.1	0.8	< 0.5	0.7	0.16	1.116
477695	< 5	80	0.399	< 0.2	259	< 1	2.5	183	< 3	23	55	162	12.1	1.2	< 0.5	2.4	0.35	1.230
477696	28	30	0.040	< 0.2	87	< 1	6.3	10	< 3	56	324	357	33.7	1.4	1.3	6.2	0.87	1.349
477697	< 5	< 20	3.930	< 0.2	154	< 1	0.5	181	< 3	7	114	19	3.6	0.3	< 0.5	0.7	0.10	1.250
488101	< 5	30	0.017	< 0.2	173	< 1	2.4	20	< 3	2	32	103	12.5	0.6	< 0.5	0.4	< 0.05	1.144
488102	< 5	< 20	0.023	< 0.2	175	< 1	< 0.5	323	< 3	23	86	55	4.6	1.2	< 0.5	2.4	0.35	1.429

*Methods: F = fusion inductively coupled plasma mass spectrometry (ICP-MS); I = instrumental neutron activation analysis (INNA); T = 'total' four-acid digestion-ICP.

APPENDIX C. – ‘Research grade’ trace element analyses

Appendix C. 'Research grade' trace element analyses

	V	Cr	Co	Ni	Cu	Zn	Ga	Ge	As	Rb	Sr	Y	Zr	Nb	Ag	Sn	Sb	Cs	Ba
Conc.	ppm	ppm	ppm	ppm	ppm	ppm	ppm	ppm	ppm	ppm	ppm	ppm	ppm	ppm	ppm	ppm	ppm	ppm	ppm
Det. Lim.	5	20	1	20	10	30	1	0.5	5	1	2	0.5	1	0.2	0.5	1	0.2	0.1	3
Method*	F	F	F	F	F	F	F	F	F	F	F	F	F	F	F	F	F	F	F
477621	225	280	53	160	60	90	16	1.6	< 5	5	98	20.8	34	0.6	0.8	< 1	< 0.2	< 0.1	62
477622	148	40	22	30	20	70	18	1.1	< 5	37	291	16.1	124	5.7	< 0.5	1	< 0.2	1.0	381
477624	122	330	20	< 20	50	390	17	0.7	< 5	97	76	19.7	125	4.3	< 0.5	< 1	< 0.2	1.8	1380
477625	209	< 20	32	< 20	120	340	15	1.2	< 5	67	3	45.2	209	7.1	< 0.5	6	< 0.2	1.2	486
477627	35	< 20	8	< 20	< 10	230	18	1.4	< 5	82	5	62.9	426	8.2	< 0.5	2	< 0.2	0.9	242
477630	55	< 20	< 1	< 20	< 10	< 30	12	0.6	< 5	11	47	23.1	275	10.4	< 0.5	2	< 0.2	< 0.1	670
477631	96	190	23	80	20	70	18	0.9	< 5	55	184	14.7	156	5.0	< 0.5	1	< 0.2	1.1	486
477634	110	220	13	50	20	170	17	1.1	< 5	10	191	17.6	163	5.4	< 0.5	1	< 0.2	0.2	178
477635	109	230	8	50	50	< 30	11	0.6	< 5	8	62	14.0	189	6.4	< 0.5	7	< 0.2	0.1	277
477637	147	80	24	30	20	100	17	1.0	< 5	79	35	29.0	149	4.9	< 0.5	2	< 0.2	1.0	395
477638	142	20	25	30	40	130	17	0.9	< 5	69	105	24.0	152	5.4	< 0.5	1	2.9	1.2	563
477639	183	110	24	40	80	450	19	1.1	< 5	70	23	27.3	174	6.1	< 0.5	1	< 0.2	1.0	357
477641	5	< 20	8	< 20	20	50	17	0.9	< 5	119	68	38.4	308	7.7	< 0.5	2	< 0.2	3.1	561
477642	92	130	20	60	90	560	19	1.1	< 5	55	56	16.8	171	5.9	< 0.5	3	< 0.2	0.9	531
477643	80	100	19	60	< 10	80	18	1.1	< 5	50	175	14.7	155	5.5	< 0.5	2	< 0.2	0.7	744
477644	94	160	19	50	40	130	18	1.4	< 5	104	55	16.5	170	5.5	< 0.5	4	< 0.2	1.2	598
477652	143	2110	74	620	< 10	30	8	4.7	< 5	2	28	8.3	17	0.6	< 0.5	3	0.9	< 0.1	16
477653	226	380	49	150	20	80	16	1.5	< 5	64	147	19.2	58	1.4	< 0.5	< 1	< 0.2	3.5	128
477654	270	< 20	22	< 20	40	130	26	1.6	< 5	2	380	29.3	136	9.4	< 0.5	6	< 0.2	< 0.1	162
477660	116	1400	68	310	490	40	74	7.2	< 5	3	39	6.9	11	0.7	< 0.5	3	< 0.2	< 0.1	116
477661	147	4080	87	1040	< 10	50	8	4.4	< 5	4	18	7.7	16	0.5	< 0.5	2	0.6	0.1	15
477665	167	30	27	50	< 10	90	20	1.2	< 5	71	640	19.5	139	6.6	< 0.5	1	0.3	0.9	789
477669	295	450	54	110	70	70	16	1.6	< 5	5	94	12.8	42	1.6	< 0.5	< 1	< 0.2	< 0.1	103
477670	153	20	26	40	10	80	19	1.1	< 5	47	709	15.6	114	4.6	< 0.5	1	< 0.2	1.0	744
477676	32	< 20	16	< 20	20	200	26	0.9	< 5	122	26	65.7	534	14.8	< 0.5	7	< 0.2	1.6	515
477677	140	50	19	40	10	80	16	1.1	< 5	62	246	14.7	109	4.2	< 0.5	< 1	< 0.2	2.0	548
477682	173	40	18	40	70	50	18	1.2	< 5	59	166	17.5	136	5.1	< 0.5	1	< 0.2	1.5	462
477683	38	< 20	43	70	610	30	15	0.6	15	41	56	34.6	203	7.5	< 0.5	2	0.3	0.8	520
477684	< 5	< 20	2	< 20	30	< 30	9	0.6	< 5	6	122	10.3	440	0.5	< 0.5	< 1	< 0.2	0.1	115
477685	158	260	36	110	190	140	18	1.2	< 5	174	102	15.2	136	4.5	< 0.5	2	< 0.2	7.6	321
477686	141	320	55	150	780	70	18	1.6	< 5	100	80	28.2	244	5.7	< 0.5	2	0.4	1.8	649
477691	115	380	31	130	< 10	120	19	1.1	< 5	105	291	17.7	147	5.4	< 0.5	1	< 0.2	2.9	462
477692	131	80	14	< 20	610	70	20	1.4	< 5	73	187	25.2	200	6.9	0.9	1	< 0.2	1.7	273
488101	20	< 20	4	< 20	< 10	40	22	1.1	< 5	38	177	3.7	105	2.2	< 0.5	< 1	0.9	5.5	429

*Method: F = fusion inductively coupled plasma mass spectrometry (ICP-MS).

Appendix C. 'Research grade' trace element analyses (continued)

	La	Ce	Pr	Nd	Sm	Eu	Gd	Tb	Dy	Ho	Er	Tm	Yb	Lu	Hf	Ta	W	Tl	Pb	Th	U
Conc.	ppm	ppm	ppm	ppm	ppm	ppm	ppm	ppm	ppm	ppm	ppm	ppm	ppm	ppm	ppm	ppm	ppm	ppm	ppm	ppm	ppm
Det. Lim.	0.1	0.05	0.01	0.05	0.01	0.005	0.01	0.01	0.01	0.01	0.01	0.005	0.01	0.002	0.1	0.01	0.5	0.05	5	0.05	0.01
Method*	F	F	F	F	F	F	F	F	F	F	F	F	F	F	F	F	F	F	F	F	F
477621	2.3	5.77	0.86	4.55	1.44	0.600	2.13	0.46	3.28	0.72	2.26	0.348	2.32	0.375	1.1	0.03	< 0.5	< 0.05	< 5	0.24	0.11
477622	17.6	33.30	3.86	15.90	3.32	1.130	3.16	0.54	3.13	0.60	1.71	0.246	1.57	0.240	3.0	0.44	< 0.5	0.22	8	2.03	0.61
477624	19.4	38.10	4.34	17.30	3.41	1.060	3.25	0.55	3.33	0.68	2.14	0.334	2.22	0.336	3.1	0.35	0.5	0.75	17	4.43	0.77
477625	22.8	42.90	4.47	16.90	3.02	0.506	4.67	1.23	8.14	1.53	4.44	0.641	4.05	0.613	5.5	0.52	< 0.5	0.44	< 5	6.44	0.49
477627	39.6	77.50	8.74	34.10	7.40	1.500	8.08	1.65	10.30	2.08	6.17	0.933	5.92	0.885	10.7	0.67	< 0.5	0.43	13	11.30	2.28
477630	39.4	73.20	7.88	30.00	5.48	1.390	4.35	0.71	4.01	0.76	2.31	0.345	2.27	0.357	7.0	1.07	6.9	< 0.05	< 5	11.00	1.71
477631	20.5	39.80	4.43	16.60	3.13	0.901	2.65	0.45	2.59	0.50	1.46	0.212	1.34	0.197	3.7	0.44	< 0.5	0.30	8	4.73	0.65
477634	24.0	46.80	5.28	20.00	3.55	1.060	3.05	0.52	3.04	0.61	1.78	0.262	1.71	0.273	4.0	0.53	< 0.5	0.24	15	6.33	1.20
477635	18.1	33.20	3.53	12.60	2.32	1.040	2.06	0.37	2.32	0.46	1.37	0.213	1.40	0.213	4.5	0.62	4.7	0.06	< 5	6.28	0.73
477637	18.1	35.50	3.99	16.10	3.43	0.820	4.14	0.87	5.29	1.01	3.04	0.462	3.00	0.455	4.0	0.39	< 0.5	0.47	< 5	5.22	0.67
477638	16.8	33.50	3.90	16.00	3.64	1.340	3.83	0.68	4.15	0.82	2.41	0.365	2.41	0.379	3.8	0.45	< 0.5	0.46	12	3.94	0.73
477639	19.7	39.10	4.44	17.90	3.98	0.994	4.42	0.84	4.90	0.97	2.89	0.440	2.90	0.438	4.6	0.48	< 0.5	0.42	< 5	5.61	0.75
477641	30.8	61.10	6.69	25.70	5.34	1.580	5.25	0.99	6.33	1.30	3.98	0.603	3.91	0.606	7.7	0.58	< 0.5	0.70	6	9.07	1.24
477642	23.6	43.60	4.75	18.10	3.28	0.870	3.02	0.52	2.98	0.56	1.67	0.254	1.64	0.235	4.4	0.51	< 0.5	0.38	8	6.76	0.93
477643	21.6	39.90	4.36	16.70	3.21	0.959	2.78	0.46	2.67	0.51	1.48	0.216	1.39	0.216	3.9	0.59	< 0.5	0.37	30	6.38	1.43
477644	21.1	39.90	4.32	16.40	3.04	0.789	2.55	0.46	2.78	0.55	1.59	0.230	1.46	0.225	4.1	0.44	< 0.5	0.72	7	6.36	0.76
477652	1.1	2.61	0.37	2.09	0.74	0.307	0.95	0.20	1.40	0.31	0.98	0.153	0.99	0.146	0.5	0.04	3.8	< 0.05	< 5	0.09	0.11
477653	3.4	8.63	1.25	6.38	1.99	0.986	2.51	0.50	3.27	0.68	2.01	0.303	1.99	0.308	1.5	0.11	< 0.5	0.33	< 5	0.36	0.15
477654	16.8	43.20	6.01	28.30	7.05	2.400	6.91	1.14	6.19	1.13	3.02	0.409	2.52	0.369	3.8	0.75	0.9	< 0.05	< 5	0.49	0.15
477660	2.4	6.92	0.79	2.96	0.70	0.248	0.89	0.16	1.05	0.23	0.72	0.109	0.71	0.112	0.3	0.03	73.0	0.06	< 5	0.06	0.02
477661	0.9	2.66	0.38	2.04	0.66	0.247	0.90	0.18	1.28	0.28	0.88	0.136	0.91	0.143	0.5	0.04	1.4	< 0.05	< 5	0.31	0.11
477665	57.6	121.00	13.50	51.00	7.85	2.320	5.34	0.72	3.74	0.71	2.06	0.291	1.76	0.248	3.3	0.60	< 0.5	1.01	10	7.28	0.98
477669	3.7	8.73	1.13	5.22	1.51	0.650	1.77	0.36	2.31	0.47	1.37	0.204	1.32	0.196	1.2	0.16	1.1	0.39	< 5	0.64	0.36
477670	46.6	103.00	12.00	46.60	7.20	2.230	4.80	0.62	3.28	0.61	1.70	0.241	1.49	0.209	2.9	0.26	< 0.5	4.33	7	5.09	0.35
477676	57.9	114.00	12.50	48.00	10.10	1.410	9.72	1.85	11.10	2.30	7.27	1.110	7.14	1.110	13.8	0.78	< 0.5	0.72	11	16.10	1.90
477677	16.2	31.60	3.40	13.50	2.75	0.921	2.54	0.43	2.64	0.53	1.55	0.227	1.42	0.220	2.9	0.37	1.9	0.39	7	3.21	0.60
477682	17.9	33.40	3.90	15.30	3.25	1.000	3.34	0.55	3.07	0.62	1.84	0.275	1.77	0.282	3.6	0.43	< 0.5	0.35	< 5	2.97	0.60
477683	26.3	50.30	5.87	22.60	4.91	1.010	5.53	0.95	5.56	1.11	3.37	0.491	3.03	0.454	5.2	0.86	5.1	0.23	5	11.10	1.62
477684	25.5	44.40	4.79	16.80	3.07	0.622	2.74	0.37	1.78	0.33	0.95	0.143	0.97	0.166	12.3	0.03	< 0.5	< 0.05	7	8.78	0.69
477685	12.3	23.60	2.78	10.80	2.39	0.866	2.55	0.44	2.55	0.51	1.57	0.245	1.62	0.244	3.4	0.37	0.8	1.07	7	3.87	0.73
477686	22.4	40.90	4.56	17.30	3.77	0.959	4.58	0.85	4.94	0.91	2.69	0.412	2.73	0.432	6.0	0.49	0.6	0.48	< 5	6.60	0.71
477691	16.2	31.90	3.73	14.50	3.18	0.877	3.17	0.53	3.09	0.60	1.72	0.244	1.53	0.236	3.7	0.45	0.6	0.67	15	4.95	0.84
477692	18.5	33.90	3.90	14.60	3.07	0.813	3.30	0.60	3.85	0.79	2.38	0.367	2.37	0.368	4.8	0.53	0.9	0.57	10	5.98	0.96
488101	11.2	21.70	2.20	7.64	1.28	0.551	0.94	0.13	0.63	0.12	0.34	0.053	0.34	0.048	2.7	0.23	2.0	0.26	6	3.32	0.95

*Method: F = fusion inductively coupled plasma mass spectrometry (ICP-MS).

APPENDIX D. – Residual soil analyses

Appendix D. Residual soil analyses

Element				Au	Ag	Cu	Cd	Mo	Pb	Ni	Zn	S	Al	As	Ba
Conc.				ppb	ppm	ppm	ppm	ppm	ppm	ppm	ppm	%	%	ppm	ppm
Det. Lim.				2	0.3	1	0.3	1	3	1	1	0.01	0.01	0.5	50
	Location, UTM east, north		Method*	I	M	T	T	T	T	M	M	T	T	I	I
507929	2006aag 271	494728	7173439	270	3.9	274	0.4	6	12	11	89	1.78	4.87	< 0.5	740
507930	2006aag 267	494599	7172821	44	1.6	100	< 0.3	15	12	66	82	0.11	5.19	< 0.5	300
507931	2006aag 020	494898	7186140	32	3.6	88	0.4	26	29	14	203	1.77	5.31	0.6	590
507932	2006aag 080	495435	7186710	214	4.8	339	0.3	5	205	40	301	1.58	3.89	< 0.5	940
507933	2006aag 080	495435	7186710	82	3.8	87	0.5	1	93	32	538	0.47	5.59	< 0.5	450
507934	2006aag 083	495415	7187043	5360	1.1	544	< 0.3	2	13	14	119	2.75	3.03	< 0.5	400
507935	2006aag 083	495415	7187043	84	3.2	126	< 0.3	3	15	21	119	0.42	4.77	< 0.5	470
507936	2006aag 092	496674	7192730	< 2	1.0	13	< 0.3	2	19	30	47	0.05	3.89	< 0.5	420
507937	2006aag 092	496674	7192730	< 2	1.4	17	< 0.3	2	14	31	39	0.06	4.24	< 0.5	420
507938	2006aag 092	496674	7192730	7	1.0	57	< 0.3	1	17	55	69	0.03	4.95	< 0.5	530
507939	2006aag 112	492194	7190913	< 2	1.0	132	< 0.3	5	10	152	62	0.06	4.86	< 0.5	320
507940	2006aag 118	492564	7191416	134	1.4	330	0.3	7	15	22	88	0.27	5.76	< 0.5	360
507941	2006aag 118	492564	7191416	429	1.2	273	0.6	9	18	12	68	0.55	2.50	< 0.5	760
507942	2006aag 134	495247	7191956	< 2	1.2	76	< 0.3	6	19	76	65	0.16	5.17	1.3	510
507943	2006aag 140	493871	7190546	< 2	1.4	165	< 0.3	3	18	57	63	0.58	5.42	< 0.5	630
507944	2006aag 153	493331	7190482	138	3.9	142	< 0.3	8	23	51	63	0.81	5.51	< 0.5	490
507945	2006aag 161	493629	7192089	37	1.6	118	< 0.3	2	10	34	56	0.97	6.23	< 0.5	370
507946	2006aag 165	494043	7192756	19	1.7	36	< 0.3	4	16	61	53	0.03	5.42	< 0.5	350
507947	2006aag 167	494275	7192829	136	3.5	84	0.4	11	20	30	100	0.17	3.70	< 0.5	360
507948	2006aag 180	496290	7189175	< 2	2.4	60	< 0.3	3	18	26	90	0.14	3.85	< 0.5	310
507949	2006aag 181	496262	7188876	57	3.3	77	< 0.3	6	42	2	124	0.54	5.06	1.4	460
507950	2006aag 195	493108	7189501	< 2	0.9	79	< 0.3	9	14	60	59	0.12	4.66	< 0.5	< 50

Element	Br	Ca	Co	Cr	Cs	Eu	Fe	Hf	Hg	Ir	K	Mg	Mn	Na	P	Rb
Conc.	ppm	%	ppm	ppm	ppm	ppm	%	ppm	ppm	ppb	%	%	ppm	%	%	ppm
Det. Lim.	0.5	0.01	1	2	1	0.2	0.01	1	1	5	0.01	0.01	1	0.01	0.001	15
Method*	I	T	I	I	I	I	I	I	I	I	T	T	T	I	T	I
507929	16.1	1.70	4	99	3	1.4	12.60	11	< 1	< 5	2.75	1.64	570	1.53	0.091	128
507930	14.4	3.34	20	225	< 1	1.4	7.79	9	< 1	< 5	1.46	1.98	1230	2.30	0.070	< 15
507931	6.8	1.68	3	135	2	1.3	9.82	12	< 1	< 5	2.98	2.99	1300	1.28	0.045	83
507932	5.8	1.81	2	414	< 1	1.2	15.40	12	< 1	< 5	2.62	2.23	1240	0.69	0.028	67
507933	20.4	2.39	8	189	< 1	1.3	6.39	10	< 1	< 5	1.47	1.79	1070	1.59	0.059	< 15
507934	3.1	0.49	9	315	< 1	1.2	17.30	9	< 1	< 5	2.95	1.77	800	0.56	0.014	59
507935	29.8	1.92	7	117	< 1	1.4	7.13	9	< 1	< 5	1.50	1.77	723	1.69	0.042	60
507936	18.7	2.77	10	86	1	0.9	3.26	9	< 1	< 5	1.20	0.90	689	2.34	0.060	< 15
507937	23.8	2.87	9	82	1	1.1	2.86	10	< 1	< 5	1.18	0.91	533	2.37	0.038	< 15
507938	23.8	3.41	20	126	< 1	1.5	5.07	10	< 1	< 5	1.20	1.42	899	2.48	0.068	71
507939	7.7	3.56	19	450	< 1	0.9	6.26	9	< 1	< 5	1.21	1.89	762	2.24	0.051	< 15
507940	15.3	1.47	7	378	2	0.4	16.60	3	< 1	< 5	1.10	2.87	841	1.92	0.014	< 15
507941	6.1	0.83	3	270	< 1	< 0.2	22.90	3	< 1	< 5	0.98	2.03	579	1.67	0.009	63
507942	16.1	3.09	14	315	2	1.1	7.83	9	< 1	< 5	1.30	1.47	659	2.30	0.050	< 15
507943	22.1	3.79	11	261	< 1	0.9	10.10	8	< 1	< 5	1.60	1.97	713	2.11	0.061	60
507944	10.2	4.42	10	324	2	1.0	12.90	5	< 1	< 5	1.49	2.45	733	1.56	0.040	111
507945	10.2	3.16	9	324	2	0.7	10.80	8	< 1	< 5	2.27	3.99	736	1.58	0.063	102
507946	18.6	3.41	18	161	< 1	1.0	3.93	11	< 1	< 5	1.36	1.49	724	2.45	0.035	< 15
507947	8.8	4.15	6	291	< 1	< 0.2	20.90	5	< 1	< 5	0.57	2.09	1000	1.54	0.033	< 15
507948	19.4	2.40	7	76	< 1	1.0	4.00	15	< 1	< 5	1.55	0.97	517	2.28	0.024	< 15
507949	19.2	1.43	< 1	49	3	1.0	13.30	12	< 1	< 5	1.96	1.82	456	1.92	0.071	< 15
507950	20.8	3.66	13	282	2	0.6	7.51	7	< 1	< 5	1.06	1.77	658	2.22	0.050	< 15

Element	Sb	Sc	Sr	Ta	Ti	Th	U	V	W	Y	La	Ce	Nd	Sm	Sn	Tb	Yb	Lu	Mass
Conc.	ppm	ppm	ppm	ppm	%	ppm	ppm	ppm	ppm	ppm	ppm	ppm	ppm	ppm	%	ppm	ppm	ppm	g
Det. Lim.	0.1	0.1	1	0.5	0.01	0.2	0.5	2	1	1	0.5	3	5	0.1	0.01	0.5	0.2	0.05	
Method*	I	I	T	I	T	I	I	T	I	T	I	I	I	I	I	I	I	I	
507929	< 0.1	17.9	142	1.0	0.82	15.3	1.6	95	< 1	22	33.2	70	18	4.1	< 0.01	< 0.5	1.6	0.41	5.84
507930	< 0.1	17.9	240	< 0.5	0.63	7.8	1.2	130	< 1	38	33.2	84	26	5.1	< 0.01	< 0.5	2.6	0.63	5.29
507931	< 0.1	16.1	130	< 0.5	0.53	23.8	1.8	115	< 1	19	58.7	128	37	6.9	< 0.01	< 0.5	1.7	0.50	5.42
507932	< 0.1	27.2	153	< 0.5	0.63	18.7	1.8	198	< 1	16	93.5	196	60	8.5	< 0.01	< 0.5	1.0	0.38	5.27
507933	0.2	11.1	242	< 0.5	0.42	11.9	2.1	119	3	17	45.0	94	30	5.8	< 0.01	< 0.5	0.9	0.26	5.71
507934	< 0.1	12.8	87	< 0.5	0.58	14.4	1.7	217	< 1	3	49.3	111	32	6.2	< 0.01	< 0.5	0.5	< 0.05	4.94
507935	< 0.1	12.8	218	< 0.5	0.45	13.6	2.1	115	< 1	16	43.3	102	32	6.0	< 0.01	1.0	2.1	0.46	5.54
507936	< 0.1	11.1	336	< 0.5	0.34	5.4	< 0.5	83	< 1	11	16.1	43	9	2.9	< 0.01	< 0.5	1.2	0.26	6.27
507937	< 0.1	11.1	326	< 0.5	0.31	5.8	1.4	80	3	17	39.1	78	26	4.6	< 0.01	< 0.5	1.3	0.34	5.72
507938	< 0.1	16.1	349	< 0.5	0.43	12.8	2.4	115	< 1	23	51.8	128	53	6.2	< 0.01	< 0.5	1.8	0.39	2.89
507939	< 0.1	16.1	304	1.7	0.46	4.7	1.1	124	< 1	16	16.1	38	14	3.0	< 0.01	< 0.5	1.2	0.31	6.05
507940	< 0.1	23.0	211	< 0.5	0.43	3.5	< 0.5	234	6	8	7.7	20	< 5	1.2	< 0.01	< 0.5	0.7	0.16	5.99
507941	< 0.1	26.4	152	< 0.5	0.49	2.6	< 0.5	310	27	< 1	7.7	20	< 5	0.9	< 0.01	< 0.5	0.4	0.09	6.28
507942	< 0.1	17.9	323	< 0.5	0.52	5.4	4.8	143	< 1	18	15.3	46	14	3.3	< 0.01	< 0.5	1.4	0.28	5.71
507943	< 0.1	19.5	276	2.4	0.75	7.7	1.9	222	< 1	15	16.1	38	9	2.8	< 0.01	< 0.5	1.2	0.31	5.62
507944	< 0.1	26.4	235	< 0.5	1.44	2.4	< 0.5	353	< 1	21	10.2	29	12	2.7	< 0.01	< 0.5	1.6	0.40	5.97
507945	< 0.1	15.3	220	1.3	0.77	1.9	0.6	206	< 1	17	10.2	23	9	2.1	< 0.01	< 0.5	0.9	0.22	6.23
507946	< 0.1	13.2	368	< 0.5	0.38	5.0	1.8	103	< 1	22	35.3	77	16	4.0	< 0.01	0.7	1.8	0.25	5.60
507947	< 0.1	28.1	194	< 0.5	0.92	2.2	< 0.5	351	< 1	6	6.9	15	< 5	1.4	< 0.01	< 0.5	1.2	0.17	5.71
507948	0.4	10.2	272	< 0.5	0.31	8.6	2.5	67	< 1	15	30.5	56	22	4.9	< 0.01	< 0.5	1.8	0.28	5.85
507949	0.3	24.6	145	2.2	0.80	15.0	< 0.5	233	< 1	15	38.2	68	25	4.9	< 0.01	< 0.5	2.4	0.34	5.65
507950	< 0.1	19.7	253	< 0.5	0.38	3.4	< 0.5	140	< 1	14	17.4	34	15	2.7	< 0.01	< 0.5	1.3	0.18	5.76

*Methods: F = fusion inductively coupled plasma mass spectrometry (ICP-MS); I = instrumental neutron activation analysis (INNA); M = Multi INNA/'total' four-acid digestion-ICP; T = 'total' four-acid digestion-ICP.